CORRELATION OF THE SOLUBILIZING ABILITIES OF 1-BUTYL-1-METHYL-PYRROLIDINIUM *TRIS*(PENTAFLUOROETHYL)TRIFLUOROPHOSPHATE, 1-BUTYL-1-METHYLPYRROLIDINIUM TRIFLATE AND 1-METHOXYETHYL-1-METHYLMORPHOLINIUM *TRIS*(PENTAFLUOROETHYL)TRIFLUOROPHOSPHATE

Pamela Twu[a], Jared L. Anderson[a], Timothy W. Stephens[b], Anastasia Wilson[b], William E. Acree, Jr.[b] and Michael H. Abraham[c]

[a] Department of Chemistry, The University of Toledo, 2801 W. Bancroft Street MS 602, Toledo, OH 43606 (USA)

[b] Department of Chemistry, 1155 Union Circle Drive #305070, University of North Texas, Denton, TX 76203-5017 (USA)

[c] Department of Chemistry, University College London, 20 Gordon Street, London, WC1H 0AJ (UK)

Abstract

Chromatographic retention data were measured for a wide range of organic solutes on 1-butyl-1-methylpyrolidinium *tris*(pentafluoroethyl)trifluorophosphate, ($[BMPyrr]^+$ $[FAP]^-$) and 1-butyl-1-methylpyrrolidinium triflate, ($[BMPyrr]^+[Trif]^-$) and 1-methoxyethyl-1-methylmorpholinium *tris*(pentafluoroethyl)trifluorophosphate, ($[MeoeMMorp]^+[FAP]^-$), stationary phases at 323 K, 353 K and 383 K. The measured retention factors were combined with published infinite dilution activity coefficient and gas-to-water partition coefficient data to yield gas-to-anhydrous ionic liquid (IL) and water-to-anhydrous IL partition coefficients. The three sets of partition coefficients were analyzed using the Abraham model. The derived Abraham model correlations

describe the observed gas-to-IL ($\log_{10} K$) and water-to-IL ($\log_{10} P$) partition coefficient data to within average standard deviations of about 0.11 and 0.15 $\log_{10}$ units, respectively.

Key Words and Phrases:

Chromatographic retention factors, partition coefficients, ionic liquids, activity coefficients, linear free energy relationships

---

*To whom correspondence should be addressed. (E-mail: acree@unt.edu)

Introduction

Ionic liquids (ILs) have been known for more than 50 years now; however, the application of ILs as solvent media in industrial manufacturing and chemical separation processes has experienced tremendous growth during the last decade. The increased applications have resulted because ILs exhibit high thermal stability and negligible vapor pressures. Ravilla and Banerjee [1] recently investigated 1-ethyl-3-methylimidazolium methylsulfonate, 1-ethyl-3-methylimida-zolium ethylsulfate and 1-ethyl-3-methylimidazolium acetate as green solvents for the denitrification of diesel oil at T = 298.15 K and atmospheric pressure. Chen and coworkers [2] synthesized four thiazolium-based ILs (i.e., 3-butyl-4-methylthiazolium dicyanamide, 3-butyl-4-methylthiazolium thiocyanate, 3-butyl-4-methylthiazolium hexafluorophosphate and 3-butyl-4-methylthiazolium tetrafluoroborate) for use in extractive desulfurization of fuel oils. The authors reported that a 64 % dibenzothiophene and 45 % thiophene removal could be achieved using 3-butyl-4-methylthiazolium dicyanamide. Yu et al. [3] explored the deep oxidative desulfurization of diesel fuels by functional acidic ILs. In the latter application the ILs were used as both extractant and catalyst. Task specific ionic liquids [4] and recyclable ionic liquid catalytic systems [5-9] have been used as solvent media in chemical syntheses. Most (if not all) of the named synthetic methods have been performed in ILs.

Ionic liquids are molten salts, typically composed of a bulky organic cation structure (alkylimidazolium, alkylpyridinium, alkylpyrrolidinium, alkylpiperidinium, tetraalkylphospho-nium, tetraalkylammonium) of low symmetry and either an inorganic anion (tetrafluoroborate, hexafluoroborate, nitrate, thiocyanate) or organic anion (alkylsulfate, dialkylphosphate, *bis*(trifluoromethylsulfonyl)imide, *tris*(pentafluoroethyl)trifluorophosphate). The cation type and size/symmetry affect the IL's melting point temperature, while the anion controls the extent to

which the IL is miscible with water. Judicious selection of the cation-anion pair, combined with introduction of functional groups to the IL, enables one to design ILs possessing the specific physical and chemical properties needed for a given application.

The solvation parameter model, developed by Abraham and coworkers [10,11], has been successfully employed to evaluate the solubilizing properties of a large number of traditional organic solvents [12-17] and several classes of ILs [18-33]. The solvation parameter model is based on two liner free energy relationships (LFERs), the first relationship describes solute transfer between two condensed phases:

$$\log_{10} P = c_p + e_p \cdot \mathbf{E} + s_p \cdot \mathbf{S} + a_p \cdot \mathbf{A} + b_p \cdot \mathbf{B} + v_p \cdot \mathbf{V} \quad (1)$$

and the second relationship involves solute transfer from the gas phase to a condensed phase

$$\log_{10} K = c_k + e_k \cdot \mathbf{E} + s_k \cdot \mathbf{S} + a_k \cdot \mathbf{A} + b_k \cdot \mathbf{B} + l_k \cdot \mathbf{L} \quad (2)$$

where P and K refer to the solute's condensed phase-to-condensed phase partition coefficient (often water-to-organic solvent partition coefficient) and gas-to-condensed phase partition coefficient, respectively. For ionic liquid solvents, Sprunger et al. [27, 34-36] further modified the basic solvation model

$$\log_{10} P = c_{p,cation} + c_{p,anion} + (e_{p,cation} + e_{p,anion}) \mathbf{E} + (s_{p,cation} + s_{p,anion}) \mathbf{S} + (a_{p,cation} + a_{p,anion}) \mathbf{A} + (b_{p,cation} + b_{p,anion}) \mathbf{B} + (v_{p,cation} + v_{p,anion}) \mathbf{V} \quad (3)$$

$$\log_{10} K = c_{k,cation} + c_{k,anion} + (e_{k,cation} + e_{k,anion}) \mathbf{E} + (s_{k,cation} + s_{k,anion}) \mathbf{S} + (a_{k,cation} + a_{k,anion}) \mathbf{A} + (b_{k,cation} + b_{k,anion}) \mathbf{B} + (l_{k,cation} + l_{k,anion}) \mathbf{L} \quad (4)$$

to include ion-specific equation coefficients. Once calculated, the ion-specific equation coefficients can be put together as a cation-anion pair to allow one to predict solute partitioning behavior into a given IL.

The independent variables in Eqns. (1) – (4) are solute-specific descriptors that have been determined for more than 5,000 different organic compounds and inorganic gases. The solute descriptors are defined as follows: **E** is the solute excess molar refraction in $cm^3\ mol^{-1}/10$ calculated from the solute's refractive index; **S** corresponds to a combined dipolarity/-polarizability descriptor; **A** and **B** describe the overall solute hydrogen-bond acidity and basicity, respectively; **V** represents McGowan's characteristic molecular volume in units of $cm^3\ mol^{-1}/100$ and **L** is the logarithm of the gas-to-hexadecane partition coefficient measured at 298 K. The set of solvent/system coefficients (c_p, e_p, s_p, a_p, b_p, v_p, c_k, e_k, s_k, a_k, b_k and l_k) characterize the transfer process and when multiplied by the respective solute descriptor measure the strength of each type of solute-condensed phase interactions. The equation coefficients are not merely fitting parameters, but represent the condensed phase properties as follows: e is a measure of the condensed phase interactions with the π- and non-bonding electrons on the solute; s measures the dipolarity/polarizability of the condensed phase; a describes the condensed phase hydrogen bond basicity (the complimentary property to solute hydrogen bond acidity) and b is the condensed phase hydrogen bond acidity (the complimentary property to solute hydrogen bond basicity). The v and l coefficients in Eqns. 1-4 reflect general dispersions that facilitate solubility of a dissolved solute and the condensed phase-condensed phase interactions that oppose the solubilization process. In the case of solute transfer between two condensed (Eqns. 1 and 3), the equation coefficients refer to differences in the properties of the condensed phases.

The advantage of characterizing solute transfer using the Abraham model is that once the equation coefficients have been calculated one can readily estimate further values of $\log_{10} P$ and $\log_{10} K$ for any additional solute for which descriptors are known. To date, we have reported IL-specific equation coefficients for 30 different ILs (Eqns. 1 and 2), and 21 cation-specific and 14 anion-specific coefficients (Eqns. 3 and 4), based on measured infinite dilution activity coefficient data, gas chromatographic retention factors and solubilities of solutes dissolved in anhydrous IL solvents [18-36]. The afore-mentioned properties are thermodynamically related to the solute's gas-to-IL and water-to-IL partition coefficients. The water-to-anhydrous IL correlations describe "hypothetical" partitions, in which the partition coefficient is calculated as the molar solubility ratio for the solute dissolved in both neat solvents. Practical partition coefficients, on the other hand, represent true equilibrium partitioning between a water-saturated organic phase and an aqueous phase that is likewise saturated with the organic solvent. Correlations derived from the Abraham model Eqns 1 and 2 described the $\log_{10} K$ and $\log_{10} P$ data for 30 different ILs to within 0.105 $\log_{10}$ units and 0.135 $\log_{10}$ units, respectively, the quoted values representing the average standard deviations of the individual correlations. Expressions based on Eqns. 3 and 4, and using our calculated ion-specific equation coefficients, predict the 3218 experimental $\log_{10} K$ (at 298 K) values, 3046 experimental $\log_{10} K$ (at 323 K) values and 3177 experimental $\log_{10}$ P (at 298 K) values in our large unpublished ion-specific partition coefficient databases to within 0.128, 0.119 and 0.151 $\log_{10}$ units, respectively. Equations 1–4 are expected to provide reasonably accurate $\log_{10} P$ and $\log_{10} K$ predictions for solutes dissolved in ILs at a given temperature (e.g., 298 K or 323 K), provided that one stays within the predictive area of chemical space defined by the solute descriptors of the compounds used in determining the equation coefficients. The area of predictive chemical space would be: **E** = 0.000 to 1.500; **S**

= 0.000 to 1.720; **A** = 0.000 to 1.040; **B** = 0.000 to 1.280; **V** = 0.109 to 1.799; and **L** = –1.200 to 7.833. A few of the IL-specific and ion-specific data sets spanned a slightly smaller range of solute descriptors.

In the present study, we report gas-liquid chromatographic retention factor data for a wide range of organic solutes on 1-butyl-1-methylpyrrolidinium *tris*(pentafluoroethyl)trifluoro-phosphate, ([BMPyrr]$^+$ [FAP]$^-$), 1-butyl-1-methylpyrrolidinium triflate, ([BMPyrr]$^+$[Trif]$^-$), and 1-methoxyethyl-1-methylmorpholinium *tris*(pentafluoroethyl)trifluorophosphate, ([MeoeMMorp]$^+$[FAP]$^-$), stationary phases at 323 K and 353 K. Results of the chromatographic measurements, combined with published infinite dilution activity coefficient data, and gas-to-liquid partition coefficient data for volatile solutes dissolved in ([BMPyrr]$^+$[FAP]$^-$) [37], ([BMPyrr]$^+$[Trif]$^-$) [38] and ([MeoeMMorp]$^+$[FAP]$^-$) [39], were used to derive Abraham model $\log_{10} K$ and $\log_{10} P$ correlations at 298 K and 323 K. We note that Wlazlo and Marciniak [39] previously reported on Abraham model correlations for ([MeoeMMorp]$^+$[FAP]$^-$) at 318, 328, 338, 348, 358 and 368 K. The datasets used in deriving the published correlations, however, did not include many of the lesser volatile organic compounds considered in the present study, and as a result the expanse of predictive chemical space covered by the published Abraham model correlations is less than that achieved by the correlations derived here.

Experimental Methods and Partition Coefficient Datasets

All ILs examined in this study were provided as gifts from Merck KGaA (Darmstadt, Germany). The ILs were coated as stationary phases onto a five meter untreated fused silica capillary columns (5 m x 0.25 mm) purchased from Supelco (Bellefonte, PA) by the static

method at 313 K. In all cases, the IL coating solutions were prepared in dichloromethane using an IL concentration of 0.45% (w/v).

Forty-two (42) probe molecules were selected for the characterization of the IL-based stationary phases. *p*-Cresol, *m*-xylene, *o*-xylene, and *p*-xylene were purchased from Fluka (Steinheim, Germany), and 1-butanol, ethyl acetate, 2-propanol, and toluene were purchased from Fisher Scientific. Acetic acid, methyl caproate, naphthalene, and propionic acid were purchased from Supelco (Bellefonte, PA, USA). Butyraldehyde and 2-nitrophenol were purchased from Acros Organics (Morris Plains, NJ, USA). Ethylbenzene was purchased from Eastman Kodak Company (Rochester, NJ, USA), cyclohexanol from J.T. Baker (Phillipsburg, NJ, USA), and the remaining solutes, namely acetophenone, benzaldehyde, benzene, benzonitrile, benzyl alcohol, 1-bromohexane, 1-bromooctane, 1-chlorobutane, 1-chlorohexane, 1-chlorooctane, cyclohexanone, 1,2-dichlorobenzene, 1,4-dioxane, 1-iodobutane, nitrobenzene, 1-nitropropane, 1-octanol, octylaldehyde, 1-pentanol, 2-pentanone, phenetole, phenol, propionitrile, pyridine, pyrrole, and 1-decanol were purchased from Sigma-Aldrich (St. Louis, MO, USA). All probe molecules had purities of greater than 98 %, and were used as received. The presence of small amounts of impurities in these solutes should in no way affect our results since the main chromatographic peak can be routinely distinguished from any impurity peak by its much higher intensity.

Chromatographic retention factors, *k*, were measured on $[BMPyrr]^+[FAP]^-$, $[BMPyrr]^+[Trif]^-$ and $[MeoeMMorp]^+[FAP]^-$ stationary phases at 323 K, 353 K and 383 K as part of the present study. Methane was used to measure the dead volume of each column at the three different temperatures. The percent relative standard deviation (% RSD) in experimental retention times for all solutes included in this study was under 1%. To ensure the integrity of the

stationary phases throughout the study, the retention factor and efficiency of naphthalene separation was periodically monitored**.** The experimental $\log_{10} k$ values are tabulated in Tables 1 - 3, respectively, along with our extrapolated 298 K $\log_{10} k$ values obtained through a $\log_{10} k$ versus 1/T linear plot of the measured data at 323 K and 353 K. The values were checked by performing the extrapolation back to 298 K using the measured data at 323 K and 383 K. A comparison of the numerical values in Tables 4 – 6 shows that the two sets of extrapolated $\log_{10} k$ (298 K) values differ by at most 0.038 $\log_{10}$ units. The majority of the calculated differences are less than 0.02 $\log_{10}$ units. We have elected to use the extrapolated $\log_{10}$ k values based on the two lower temperatures in developing our correlation equations because $\log_{10}$ k versus 1/T plots are expected to be linear over small temperature intervals. The 298 K to 353 K is the smaller of the two temperature intervals. The largest estimated uncertainty in this extrapolation should be less than 0.04 based on the comparisons given in Tables 4 – 6.

The gas-to-IL partition coefficient, K, can be obtained from isothermal chromatographic measurements through $K = V_N/V_L$ where V_N is the volume of gas required to elute a solute, and V_L is the volume of liquid present as the stationary phase [40]. The retention factor, k, is given by [40] $k = (t_r – t_m)/t_m$ where t_r is the retention time of a solute and t_m is the "void" retention time. Since $t_r – t_m$, the corrected retention time, is proportional to V_N, the corrected elution volume, it follows that gas-to-liquid partition coefficients and retention factors are interrelated,

$$K = P^* \cdot k \quad \text{or} \quad \log_{10} K = \log_{10} P^* + \log_{10} k. \qquad (5)$$

To a first approximation, the proportionality constant, P^*, is the phase ratio and depends only on chromatographic conditions that should remain constant for a given column during the time the experimental measurements are performed.

Thermodynamic gas-to-IL partition coefficients are required to calculate the proportionality constants needed in eq 8 for converting the measured $\log_{10} k$ data in Tables 1 and 2 to $\log_{10} K$ values. Dománska and coworkers measured the infinite dilution activity coefficients, γ_{solute}^{∞}, of more than 30 organic solutes in $[BMPyrr]^+[Trif]^-$ [38] at 298 K and in $[BMPyrr]^+[FAP]^-$ [37] at several temperatures ranging from 308 K to 358 K. Wlazlo and Marciniak [39] reported infinite dilution activity coefficients and gas-to-liquid partition coefficients of 62 solutes dissolved in $[MeoeMMor]^+[FAP]^-$ in the 318 to 368 K temperature range. Uncertainties in the measured K and γ_{solute}^{∞} values were reported to be on the order of 2 to 3%. In the case of $[BMPyrr]^+[FAP]^-$ and $[MeoeMMor]^+[FAP]^-$ the published experimental data were extrapolated to 298 K and 323 K by assuming a linear ln γ_{solute}^{∞} versus 1/T and linear ln K versus 1/T relationship. A linear extrapolation should be valid as the measurements were performed not too far removed from the desired temperatures (less than 20 K in most instances). The activity coefficients are converted to $\log_{10} K$ values through eq 6

$$\log_{10} K = \log_{10} \left(\frac{RT}{\gamma_{solute}^{\infty} P_{solute}^{o} V_{solvent}}\right) \quad (6)$$

and $\log_{10} P$ values for partition from water to the IL can be calculated via eq 7

$$\log_{10} P = \log_{10} K - \log_{10} K_w \quad (7)$$

In eq 6, P_{solute}^{o} is the vapor pressure of the solute at the system temperature (T), $V_{solvent}$ is the molar volume of the IL solvent, and R is the universal gas constant. The conversion of $\log_{10} K$ data to $\log_{10} P$ requires knowledge of the solute's gas phase partition coefficient into water, K_w, which is available for most of the solutes being studied. As an informational note, water-to-IL

partition coefficients (more formally called Gibbs energy of solute transfer when multiplied by –2.303 RT) calculated through eq 7 refer to a hypothetical partitioning process involving solute transfer from water to the anhydrous IL. Log_{10} *P* values calculated in this fashion are still useful in that predicted log_{10} P values can be used to estimate the solute's infinite dilution activity coefficient in the IL.

The proportionality constants needed in eq 5; log_{10} *P** = 2.802 (298 K) and log_{10} *P** = 2.790 (323 K) for $[BMPyrr]^+ [FAP]^-$, log_{10} *P** = 2,379 (298 K) and log_{10} *P** = 2.308 (323 K) for $[BMPyrr]^+ [Trif]^-$, and log_{10} *P** = 2.619 (298 K) and log_{10} *P** = 2.557 (323 K) for $[MeoeMMorp]^+[FAP]^-$, were the calculated average differences between the measured log_{10} *k* and log_{10} *K* for common compounds in the individual IL's data sets. For example, in the $[BMPyrr]^+ [FAP]^-$ data set, we determined chromatographic retention factors for thirteen compounds (i.e., acetic acid, benzene, 1-butanol, butyraldehyde, ethyl acetate, ethylbenzene, 1-nitropropane, 2-pentanone, pyridine, toluene, *m*-xylene, *o*-xylene and *p*-xylene) that had been previously studied by Dománska *et al*. The calculated log_{10} *K* and log_{10} *P* values are compiled in Tables 7 – 9 for the three ILs considered in the present study. Log_{10} *P* values are tabulated only for 298 K as we do not have experimental values for the solutes' gas phase partition coefficients into water, log_{10} K_w, at 323 K. The log_{10} K_w values that we have compiled thus far are for gas to water at 298 K [41] and 310 K [42], or for gas to physiological saline at 310 K [42]. For convenience, we have also tabulated in Table 10 the numerical values of solute descriptors for the organic compounds studied. The solute descriptors are of experimental origin, and were taken from the Abraham database. The numerical values were obtained from gas-liquid chromatographic measurements and water-to-solvent partition measurements as described in detail elsewhere [11, 43, 44].

Results and Discussion

We have assembled in Table 7 experimental $\log_{10} K$ values for 91 organic solutes and experimental $\log_{10} P$ values for 90 organic compounds in $[BMPyrr]^+[FAP]^-$ spanning a wide range of polarity and hydrogen-bonding characteristics. Preliminary analysis of the experimental data in accordance with eqs 1 and 2 of the Abraham general solvation parameter model revealed that the e_k coefficient ($e_k = 0.025 \pm 0.084$ and 0.040 ± 0.067) was negligible in both the $\log_{10} K$ (298 K) and $\log_{10} K$ (323 K) correlation. The $e_k \cdot \mathbf{E}$ term was thus eliminated from the 298 K and 323 K $\log_{10} K$ correlations, and the regression analyses were rerun to give the following three linear free energy relationships (LFERs)

$$\log_{10} K\,(298) = -0.196\,(0.062) + 2.288(0.057)\,\mathbf{S} + 1.078(0.084)\,\mathbf{A} + 0.505(0.091)\,\mathbf{B} + 0.649(0.017)\,\mathbf{L} \quad (8)$$

(N = 90, SD = 0.127, R^2 = 0.984, F = 1304)

$$\log_{10} K\,(323) = -0.291(0.050) + 2.121(0.046)\,\mathbf{S} + 0.910(0.068)\,\mathbf{A} + 0.435(0.073)\,\mathbf{B} + 0.560(0.013)\,\mathbf{L} \quad (9)$$

(N = 91, SD = 0.103, R^2 = 0.987, F = 1614)

$$\log_{10} P\,(298) = 0.100(0.096) + 0.227(0.097)\,\mathbf{E} + 0.392(0.111)\,\mathbf{S} - 2.607(0.108)\,\mathbf{A} - 4.285(0.128)\,\mathbf{B} + 3.245(0.080)\,\mathbf{V} \quad (10)$$

(N = 90, SD = 0.156, R^2 = 0.991, F = 1827)

where the standard errors in the calculated equation coefficients are given in parentheses. The statistical information associated with each correlation includes the number of experimental data points (N), the standard deviation (SD), the squared correlation coefficient (R^2) and the Fisher F-

statistic (F). All regression analyses were performed using SPSS statistical software. The LFERs described by eqs 8 – 10 are statistically very good with standard deviations of less than 0.160 $\log_{10}$ units. One small change that we have made in the present study concerns converting the measured $\log_{10} K$ value to $\log_{10} P$. We are now using a recent value of $\log_{10} K_w = -0.77$ for cyclooctane [45] in the $\log_{10} K$ to $\log_{10} P$ conversions, which is a departure from our past studies. Stephens et al. [32] noted that the value of $\log_{10} K_w = -0.77$ for cyclooctane led to slightly smaller standard deviations in the $\log_{10} P$ correlations of 1-butyl-1-methylpyrolidinium tetracyanoborate and 1-butyl-1-methyl-piperidinium *bis*(trifluoromethylsulfonyl)imide. The standard deviations in the derived correlations are slightly larger than the uncertainty in the measured data, which we estimate to be on the order of ± 0.07 to 0.10 $\log_{10}$ units. Our estimated uncertainty includes not only the uncertainties in the measured K and γ_{solute}^{∞} data, but also the uncertainties involved in extrapolating the measured values to 298 K and in the calculated proportionality constant, P^*, needed to convert the chromatographic retention factors to gas-to-liquid partition coefficients.

All three equations can be used to predict infinite dilution activity coefficients and chromatographic retention factors of solutes in anhydrous $[BMPyrr]^+[FAP]^-$. Predicted $\log_{10} K$ and $\log_{10} P$ values are converted to γ_{solute}^{∞} values through eqs 6 and 7. In the case of chromatographic retention factors, one will need to measure $\log_{10} k$ values for a few standard "calibration" solutes using the actual coated chromatographic column in order to the obtain the phase ratio (P^* in eq 8) needed to convert the predicted $\log_{10} K$ values to $\log_{10} k$ values. Figure 1 provides a plot of $\log_{10} K$ (298) values predicted from eq 8 against experimental values covering a range of approximately 4.36 $\log_{10}$ units, from $\log_{10} K = 1.056$ for pentane to $\log_{10} K = 5.421$ for *p*-cresol. A comparison of the calculated versus experimental $\log_{10} P$ data is shown in Figure 2.

As noted above, each calculated coefficient corresponds to the sum of the respective cation- and anion-specific contributions. It is possible to put together our published numerical values for the $[BMPyrr]^+$-specific ($c_{k,cation} = –0.570$; $e_{k,cation} = –0.075$; $s_{k,cation} = 2.687$; $a_{k,cation} = 2.338$; $b_{k,cation} = 0.570$ and $l_{k,cation} = 0.711$ [33]) and $[FAP]^–$-specific equation coefficients ($c_{k,anion} = 0.179$; $e_{k,anion} = –0.015$; $s_{k,anion} = 0.063$; $a_{k,anion} = –1.314$; $b_{k,anion} = 0.238$ and $l_{k,anion} = – 0.053$ [33]) to generate predictive correlations for the $[BMPyrr]^+[FAP]^–$ ionic liquid. In the case of the gas-to-$[BMPyrr]^+[FAP]^–$ the predictive correlation at 298 K is

$$\log_{10} K\,(298) = –0.393(0.091) – 0.090(0.316)\,\mathbf{E} + 2.624(0.302)\,\mathbf{S} + 1.024(0.084)\,\mathbf{A} + 0.808(0.313)\,\mathbf{B} + 0.658(0.029)\,\mathbf{L} \quad (11)$$

in reasonably good agreement with Eqn. 8 given that our existing values for the $[BMPyrr]^+$ cation were based on only 31 experimental data points. One of the reasons for performing the current study was to obtain more experimental values so that we could later revise several of the ion-specific equation coefficients that had been previously determined. We prefer not to recalculate the ion-specific equation coefficients every time that we add a few more experimental values to our large experimental $\log_{10} K$ and $\log_{10} P$ values databases. We believe that the most prudent practice would be to await on updating of the $[BMPyrr]^+$-specific equation coefficients until we have added enough new data points to make the revisions meaningful. There are several cations and anions in our data set for which we are in the process of making additional activity coefficient and retention factor measurements.

In order to assess the predictive abilities of eqs 8–10, we divided the large data sets into training sets and test sets by allowing the SPSS software to randomly select half of the experimental data points. The selected data points became the training sets and the compounds

that were left served as the test sets. Analysis of the experimental data in the two $\log_{10} K$ and single $\log_{10} P$ training sets gave

$$\log_{10} K\,(298) = -0.226(0.082) + 2.325(0.077)\,\mathbf{S} + 1.116(0.101)\,\mathbf{A} + 0.446(0.122)\,\mathbf{B} + 0.652\,(0.022)\,\mathbf{L} \quad (12)$$

(N = 45, SD = 0.115, R^2 = 0.988, F = 841)

$$\log_{10} K\,(323) = -0.337(0.051) + 2.161(0.051)\,\mathbf{S} + 0.743(0.094)\,\mathbf{A} + 0.584(0.083)\,\mathbf{B} + 0.567(0.013)\,\mathbf{L} \quad (13)$$

(N = 46, SD = 0.080, R^2 = 0.987, F = 1385)

$$\log_{10} P\,(298) = -0.087(0.135) + 0.232(0.179)\,\mathbf{E} + 0.360(0.201)\,\mathbf{S} - 2.572(0.157)\,\mathbf{A} - 4.128(0.219)\,\mathbf{B} + 3.422(0.115)\,\mathbf{V} \quad (14)$$

(N = 45, SD = 0.158, R^2 = 0.991, F = 823)

There is very little difference in the equation coefficients for the full data set and training data set correlations. The training set correlations were then used to predict the gas-to-IL partition coefficients for the 45 compounds in the $\log_{10} K$ test sets, and the water-to-IL partition coefficients of the 45 compounds in the $\log_{10} P$ test set. For the predicted and experimental values we found SD values of 0.139, 0.132 and 0.166; average absolute error (AAE) values of 0.117, 0.102 and 0.137; and average error (AE) values of 0.034, –0.046 and –0.020 for eqs 12–14, respectively, suggesting the introduction of very little bias in generating these predictions. The training and test set analyses were performed two additional times with similar results.

Experimental $\log_{10} K$ and $\log_{10} P$ values are assembled in Table 8 for organic solutes dissolved in $[BMPyrr]^+[Trif]^-$. Regression analysis of the tabulated partition coefficient data yielded the following Abraham model LFERs:

$$\log_{10} K\,(298) = -0.681(0.049) + 0.177(0.068)\,\mathbf{E} + 2.553(0.080)\,\mathbf{S} + 4.092(0.089)\,\mathbf{A} + 0.283(0.102)\,\mathbf{B} + 0.677(0.014)\,\mathbf{L} \quad (15)$$

$$(N = 66,\ SD = 0.089,\ R^2 = 0.995,\ F = 2409)$$

$$\log_{10} K\,(323) = -0.699(0.039) + 0.203(0.056)\,\mathbf{E} + 2.322(0.065)\,\mathbf{S} + 3.499(0.072)\,\mathbf{A} + 0.254(0.083)\,\mathbf{B} + 0.558(0.011)\,\mathbf{L} \quad (16)$$

$$(N = 69,\ SD = 0.094,\ R^2 = 0.995,\ F = 2751)$$

$$\log_{10} P\,(298) = -0.366(0.090) + 0.448(0.101)\,\mathbf{E} + 0.628(0.122)\,\mathbf{S} + 0.362(0.143)\,\mathbf{A} - 4.469(0.157)\,\mathbf{B} + 3.327(0.077)\,\mathbf{V} \quad (17)$$

$$(N = 65,\ SD = 0.134,\ R^2 = 0.990,\ F = 1141)$$

The derived correlations describe the observed partition coefficient data to within a standard deviation of SD = 0.14 $\log_{10}$ units for data sets covering up to 5.6 $\log_{10}$ units. See Figures 3 and 4 for a comparison of observed versus calculated values. Training and test set analyses were performed to validate the robustness of each correlation model. Comparison of the predicted test set and observed values gave SD values of 0.106, 0.068 and 0.151; AAEs of 0.085, 0.057 and 0.133; and AEs of 0.037, –0.001 and –0.028 for the $\log_{10} K$ (298), $\log_{10} K$ (323 K) and $\log_{10} P$ (298 K) equations, respectively.

Experimental $\log_{10} K$ and $\log_{10} P$ values are assembled in Table 9 for organic solutes dissolved in $[MeoeMMorp]^+[FAP]^-$. Regression analysis of the tabulated partition coefficient data yielded the following Abraham model LFERs:

$$\log_{10} K\,(298) = -0.364(0.063) + 2.645(0.060)\,\mathbf{S} + 1.319(0.095)\,\mathbf{A} + 0.887(0.093)\,\mathbf{B} + 0.595(0.017)\,\mathbf{L} \quad (18)$$

(N = 99, SD = 0.140, R^2 = 0.984, F = 1465)

$$\log_{10} K\,(323) = -0.423(0.054) + 2.444(0.051)\,\mathbf{S} + 1.172(0.080)\,\mathbf{A} + 0.696(0.079)\,\mathbf{B} + 0.503(0.015)\,\mathbf{L} \quad (19)$$

(N = 101, SD = 0.121, R^2 = 0.985, F = 1582)

$$\log_{10} P\,(298) = 0.830(0.062)\,\mathbf{S} - 2.362(0.110)\,\mathbf{A} - 4.022(0.096)\,\mathbf{B} + 3.064(0.029)\,\mathbf{V} \quad (20)$$

(N = 99, SD = 0.164, R^2 = 0.995, F = 4646)

The e·**E** term was removed from both final $\log_{10} K$ correlations, and the c and e·**E** terms were removed from the $\log_{10} P$ correlation, because they made only a very small contribution to the partition coefficient calculation. The standard deviations were unaffected by the removal of the insignificant terms. The derived correlations describe the observed partition coefficient data to within a standard deviation of about SD = 0.16 $\log_{10}$ units for data sets covering up to 6.2 $\log_{10}$ units. See Figures 5 and 6 for a comparison of observed versus calculated values.

The computational methodology that we have developed allows us to determine ion-specific equation coefficients of new cations and anions. As noted above, we have already reported $[FAP]^-$-specific equation coefficients for the $\log_{10} K$ correlation of $c_{k,anion}$ = 0.179; $e_{k,anion}$ = –0.015; $s_{k,anion}$ = 0.063; $a_{k,anion}$ = –1.314; $b_{k,anion}$ = 0.238 and $l_{k,anion}$ = – 0.053 [33] and for

the $\log_{10} P$ correlation of $c_{p,anion} = 0.132$; $e_{p,anion} = –0.171$; $s_{p,anion} = 0.121$; $a_{p,anion} = –1.314$; $b_{p,anion} = 0.244$ and $v_{p,anion} = – 0.107$ [33] based on more than 140 experimental values measured at 298 K. The cation-specific values for $[MeoeMMorp]^+$ are obtained simply by subtracting the known anion-specific values for $[FAP]^–$ from the IL-specific equation coefficients given in eqs. 18 and 20 (*e.g.*, $c_{cation} = c_{IL} – c_{anion}$; $c_{anion} = c_{IL} – c_{cation}$). Performing the subtraction we obtain $\log_{10} K$ coefficients of $c_{k,cation} = –0.543$, $e_{k,cation} = 0.015$, $s_{k,cation} = 2.582$, $a_{k,cation} = 0.005$, $b_{k,cation} = 0.649$, $l_{k,cation} = 0.648$, and $\log_{10} P$ coefficients of of $c_{p,cation} = –0.132$, $e_{p,cation} = 0.171$, $s_{p,cation} = 0.709$, $a_{p,cation} = –1.048$, $b_{p,cation} = –4.266$, $v_{p,cation} = 3.171$ for the 1-methoxyethyl-1-methylmorpholinium cation. Training and test set analyses were performed to validate the robustness of each correlation model. Comparison of the predicted test set and observed values gave SD values of 0.161, 0.135 and 0.175; AAEs of 0.127, 0.105 and 0.135; and AEs of –0.047, 0.025 and –0.020 for the $\log_{10} K$ (298), $\log_{10} K$ (323 K) and $\log_{10} P$ (298 K) equations, respectively.

Conclusions

Published infinite dilution activity coefficients, γ_{solute}^{∞}, and measured chromatographic retention factors, *k*, were combined to yield gas-to-IL partition coefficients, *K*, for organic solutes dissolved in 1-butyl-1-methylpyrolidinium *tris*(pentafluoroethyl)trifluorophosphate, ($[BMPyrr]^+[FAP]^–$) and 1-butyl-1-methylpyrrolidinium triflate, ($[BMPyrr]^+[Trif]^–$) and 1-methoxyethyl-1-methylmorpholinium *tris*(pentafluoroethyl)trifluorophosphate, ($[MeoeMMorp]^+[FAP]^-$) IL solvents. The gas-to-IL partition coefficients were converted to water-to-IL partition coefficients, *P*, using the solutes' gas-to-water partition coefficients. The three sets of partition coefficients were then analyzed using the Abraham model. The derived Abraham model correlations describe the observed gas-to-IL and water-to-IL partition

coefficient data to within average standard deviations of about 0.10 and 0.15 $\log_{10}$ units, respectively.

References

1. Ravilla, U.K., Banerjee, T.: Liquid liquid equilibria of imidazolium based ionic liquid + pyridine + hydrocarbon at 298.15 K: Experiments and correlations. Fluid Phase Equilibr. **324**, 17-27 (2012).

2. Chen, X., Liu, G., Yuan, S., Asumana, C., Wang, W., Yu, G.: Extractive desulfurization of fuel oils with thiazolium-based ionic liquids. Sep. Sci. Technol. **47**, 819-826 (2012).

3. Yu, G., Zhao, J., Song, D., Asumana, C., Zhang, X., Chaen, X.: Deep oxidative desulfurization of diesel fuels by acidic ionic liquids. Ind. Eng. Chem. Res. **50**, 11690-11697 (2011).

4. Shaterian, H.R., Honarmad, M.: Task-specific ionic liquid as the recyclable catalyst for the rapid and green synthesis of dihydropyrano[3,2-c]chromene derivatives. Synth. Comm.**41**, 3573-3581 (2011).

5. Kumar, V., Sharma, U., Verma, P. K., Kumar, N., Singh, B.: Silica-supported boric acid with ionic liquid: a novel recyclable catalytic system for one-pot three-component Mannich reaction. Chem. Pharm. Bull. **59**, 639-645 (2011).

6. Sandhu, S., Sandhu, J. S.: Recent advances in ionic liquids. Green unconventional solvents of this century. Part I. Green Chem. Lett. Reviews **4**, 289-310 (2011).

7. Sandhu, S., Sandhu, J. S.: Recent advances in ionic liquids. Green unconventional solvents of this century. Part II. Green Chem. Lett. Reviews **4**, 311-320 (2011).

8. Mukhopadhyay, C., Datta, A., Tapaswi, P.K.: Halogen-free room-temperature Bronsted acidic ionic liquid [Hmim]+ HSO_4- as a recyclable green "dual reagent" catalysis for the synthesis of triarylmethanes (TRAMS). Synthetic Comm. **42**, 2453-2463 (2012).

9. Dabiri, M., Salehi, P., Bahramnejad, M., Baghbanzadeh, M.: Eco-friendly and efficient procedure for hetero-Michael addition reactions with an acidic ionic liquid as catalyst and reaction medium. Monatsh. Chem.**143**, 109-112 (2012)**.**

10. Abraham, M.H.: Scales of solute hydrogen-bonding: their construction and application to physicochemical and biochemical processes. Chem. Soc. Reviews **22**, 73-83 (1993).

11. Abraham, M.H., Ibrahim, A., Zissimos, A.M.: Determination of sets of solute descriptors from chromatographic measurements. J. Chromatogr A 1037, 29-47 (2004).

12. Stephens, T.W., Loera, M., Quay, A.N., Chou, V., Shen, C., Wilson, A., Acree, W.E. Jr., Abraham, M.H.: Correlation of solute transfer into toluene and ethylbenzene from water and from the gas phase based on the Abraham model. Open Thermodyn. J. **5**, 104-121 (2011).

13. Saifullah, M., Ye, S., Grubbs, L.M., De La Rosa, N.E., Acree, W.E. Jr.,Abraham, M.H.: Abraham model correlations for transfer of neutral molecules to tetrahydrofuran and to 1,4-dioxane, and for transfer of ions to tetrahydrofuran. J. Solution Chem. **40**, 2082-2094 (2011).

14. Abraham, M.H., Acree, W.E. Jr.: The transfer of neutral molecules, ions and ionic species from water to benzonitrile; comparison with nitrobenzene. Thermochim. Acta **526**, 22-28 (2011).

15. Stephens, T.W., De La Rosa, N.E., Saifullah, M.,Ye, S., Chou, V., Quay, A.N., Acree, W. E. Jr., Abraham, M.H.: Abraham model correlations for transfer of neutral molecules and ions to sulfolane. Fluid Phase Equilibr. **309**, 30-35 (2011).

16. Stephens, T.W., De La Rosa, N.E., Saifullah, M., Ye, S., Chou, V., Quay, A.N., Acree, W.E. Jr.; Abraham, M.H.: Abraham model correlations for solute partitioning into o-

xylene, m-xylene and p-xylene from both water and the gas. Fluid Phase Equilibr. **308**, 64-71 (2011).

17. Abraham, M.H., Smith, R.E., Luchtefeld, R., Boorem, A.J., Luo, R., Acree, W.E. Jr.: Prediction of solubility of drugs and other compounds in organic solvents. J. Pharm. Sci. **99**, 1500-1515 (2010).

18. Acree, W.E., Jr., Abraham, M.H.: The analysis of solvation in ionic liquids and organic solvents using the Abraham linear free energy relationship. J. Chem. Technol. Biotechnol. **81**, 1441-1446 (2006). [Erratum: J. Chem. Technol. Biotechnol. **81**, 1722 (2006)]

19. Abraham, M.H., Acree, W.E., Jr.: Comparative analysis of solvation and selectivity in room temperature ionic liquids using the Abraham linear free energy relationship. Green Chem. **8**, 906-915 (2006).

20. Mintz, C., Acree, W.E., Jr.: Partition coefficient correlations for transfer of solutes from gas phase and water to room temperature ionic liquids. Phys. Chem. Liq. **45**, 241-249 (2007).

21. Sprunger, L.M.; Acree, W.E., Jr.; Abraham, M.H.: Linear free energy relationship correlations for the solubilising characterisation of room temperature ionic liquids containing 1-hexyloxymethyl-3-methylimidazolium and 1,3-dihexyloxymethyl-imidazolium cations. Phys. Chem. Liq. **48**, 394-402 (2010).

22. Moise, J.-C., Mutelet, F., Jaubert, J.-N., Grubbs, L.M., Acree, W.E., Jr., Baker, G.A.: Activity coefficients at infinite dilution of organic compounds in four new imidazolium-based ionic liquids, J. Chem. Eng. Data **56**, 3106-3114 (2011).

23. Grubbs, L.M., Ye, S., Saifullah, M., Acree, W.E., Jr., Twu, P., Anderson, J.L., Baker, G.A., Abraham, M.H.: Correlation of the solubilizing abilities of hexyl(trimethyl)-ammonium *bis*(trifluoromethylsulfonyl)imide, 1-propyl-1-methyl-piperidinium *bis*((trifluoromethyl)sulfonyl)imide and 1-butyl-1-methyl-pyrrolidinium thiocyanate, J. Solution Chem., **40**, 2000-2022 (2011).

24. Mutelet, F., Revelli, A.-L., Jaubert, J.-N., Sprunger, L.M., Acree, W.E., Jr., Baker, G.A.: Partition coefficients of organic compounds in new imidazolium and tetralkylammonium based ionic liquids using inverse gas chromatography. J. Chem. Eng. Data 55, 234-242 (2010).

25. Sprunger, L.M., Gibbs, J., Baltazar, Q.Q., Acree, W.E., Jr., Abraham, M.H., Anderson, J. L.: Characterisation of room temperature ionic liquid chromatographic stationary phases by combining experimental retention factor and partition coefficient data into a single model. Phys. Chem. Liq. 47, 74-83 (2009).

26. Revelli, A.-L., Mutelet, F., Jaubert, J.-N., Garcia-Martinez, M., Sprunger, L.M., Acree, W.E., Jr., Baker, G.A.: Study of ether-, alcohol-, or cyano-functionalized ionic liquids using inverse gas chromatography. J. Chem. Eng. Data 55, 2434-2443 (2010).

27. Grubbs, L.M., Saifullah, M., De La Rosa, N.E., Acree, W.E., Jr., Abraham, M.H., Zhao, Q., Anderson, J.L.: Cation-specific and anion-specific Abraham model correlations for solute transfer into ionic liquids. Glob. J. Phys. Chem., 1, 1-19 (2010).

28. Grubbs, L.M., Ye, S., Saifullah, M., McMillan-Wiggins, M.C., Acree, W.E., Jr., Abraham, M.H., Twu, P., Anderson, J.L.: Correlations for describing gas-to-ionic liquid partitioning at 323 K based on ion-specific equation coefficient and group contribution versions of the Abraham model. Fluid Phase Equilibr. 301,257-266 (2011).

29. Revelli, A.-L., Sprunger, L.M., Gibbs, J., Acree, W.E., Jr., Baker, G.A., Mutelet, F.: Activity coefficients at infinite dilution of organic compounds in trihexyl(tetradecyl)-phosphonium bis(trifluoromethylsulfonyl)imide using inverse gas chromatography. J. Chem. Eng. Data 54, 977-985 (2009).

30. Sprunger, L.M., Acree, W.E., Jr., Abraham, M.H.: Linear free energy relationship (LFER) correlations for the solubilising characterisation of room temperature ionic liquids containing triethylsulphonium and 1-butyl-1-methylpyrrolidinium cations, Phys. Chem. Liq. 48, 385-393 (2010).

31. Proctor, A., Sprunger, L.M., Acree, W.E., Jr., Abraham, M.H.: LFER correlations for the solubilising characterisation of room temperature ionic liquids containing trifluoro-methanesulfonate and trifluoroacetate anions. Phys. Chem. Liq. 46, 631-642 (2008).

32. Stephens, T. W., Acree, W.E. Jr., Twu, P., Anderson, J.L., Baker, G.A., Abraham, M.H.: Correlation of the solubilizing abilities of 1-butyl-1-methyl-piperidinium bis(trifluoro-methylsulfonyl)imide and 1-butyl-1-methyl-pyrrolidinium tetracyanoborate. J. Solution Chem., 41, 1165-1184 (2012).

33. Acree, W.E. Jr., Grubbs, L.M., Abraham, M.H.: Selection of Ionic Liquid Solvents for Chemical Separations Based on the Abraham Model. in Ionic Liquids, Applications and Perspectives (Book 2), Kokorin, A. (Ed.), INTECH Publishers, Chapter 13, 273-302 (2011).

34. Sprunger, L., Clark, M., Acree, W.E., Jr., Abraham, M.H.: Characterization of room-temperature ionic liquids by the Abraham model with cation-specific and anion-specific equation coefficients. J. Chem. Inf. Model. 47, 1123-1129 (2007).

35. Sprunger, L.M., Proctor, A., Acree, W.E., Jr., Abraham, M. H.: LFER correlations for room temperature ionic liquids: Separation of equation coefficients into individual cation-specific and anion-specific contributions. Fluid Phase Equilibr. 265, 104-111 (2008).

36. Sprunger, L.M., Gibbs, J., Proctor, A., Acree, W.E., Jr., Abraham, M.H., Meng, Y., Yao, C., Anderson, J.L.: Linear free energy relationship correlations for room temperature ionic liquids: revised cation-specific and anion-specific equation coefficients for predictive applications covering a much larger area of chemical space. Ind. Eng. Chem. Res. 48, 4145-4154 (2009).

37. Dománska, U., Lukoshko, E.V., M. Królikowski, M.: Measurements of activity coefficients at infinite dilution for organic solutes and water in the ionic liquid 1-butyl-1-methylpyrrolidinium *tris*(pentafluoroethyl)trifluorophosphate ([BMPYR][FAP]). Chem. Eng. J., 183, 261-270 (2012).

38. Dománska, U., Redhi, G.G., Marciniak, A.: Activity coefficients at infinite dilution measurements for organic solutes and water in the ionic liquid 1-butyl-1-methylpyrrolidinium trifluoromethanesulfonate using GLC. Fluid Phase Equilibr. 278, 97-102 (2009)]

39. Wlazlo, M., Marciniak, A.: Activity coefficients at infinite dilution and physicochemical properties for organic solutes and water in the ionic liquid 4-(2-methoxyethyl)-4-methylmorpholinium trifluorotris(perfluoroethyl)phosphate. J. Chem. Thermodyn. 54, 366-377 (2012).

40. Baltazar, Q.Q., Leininger, S.K., Anderson, J.L.: Binary ionic liquid mixtures as gas chromatography stationary phases for improving the separation selectivity of alcohols and aromatic compounds. J. Chromatogr. A **1182**, 119-127 (2008).

41. Abraham, M.H., Andonian-Haftvan, J., Whiting, G.S., Leo, A., Taft, R.W.: Hydrogen bonding. Part 34. The factors that influence the solubility of gases and vapors in water at 298 K, and a new method for its determination. J. Chem. Soc., Perkin Trans. 2 1777–1791 (1994).

42. Abraham, M.H., Ibrahim, A., Acree, W.E., Jr.: Partition of compounds from gas to water and from gas to physiological saline at 310 K: linear free energy relationships. Fluid Phase Equilibr. **251**, 93-109 (2007).

43. Zissimos, A.M., Abraham, M.H., Barker, M.C., Box, K.J., Tam, K.Y.: Calculation of Abraham descriptors from solvent-water partition coefficients in four different systems; evaluation of different methods of calculation. J. Chem. Soc., Perkin Trans. 2 470-477 (2002).

44. Zissimos, A.M., Abraham, M.H., Du, C.M., Valko, K., Bevan, C., Reynolds, D., Wood, J., Tam, K.Y.: Calculation of Abraham descriptors from experimental data from seven HPLC systems; evaluation of five different methods of calculation. J. Chem. Soc., Perkin Trans. 2 2001-2010 (2002).

45. Dohanyosova, P., Sarraute, S., Dohnal, V., Majer, V., Gomes, M.C.: Aqueous solubility and related thermodynamic functions of nonaromatic hydrocarbons as a function of molecular structure. Ind. Eng. Chem. Res. **43**, 2805-2815 (2004).

Table 1. Chromatographic retention factor data for organic solutes on a $[BMPyrr]^+[FAP]^-$ stationary phase at 298 K, 323 K, 353 K and 383 K

Solute	$\log_{10} k$ (323 K)	$\log_{10} k$ (353 K)	$\log_{10} k$ (383 K)	$\log_{10} k$ (298 K)[a]
Acetic acid	0.101	-0.457	-0.916	0.653
Acetophenone	1.789	1.103	0.560	2.466
Benzaldehyde	1.285	0.681	0.201	1.881
Benzene	-0.275	-0.748	-1.150	0.193
Benzonitrile	1.432	0.832	0.353	2.024
Benzyl alcohol	1.717	1.019	0.466	2.406
1-Bromooctane	0.648	0.069	-0.429	1.220
1-Butanol	-0.203	-0.708	-1.119	0.296
Butyraldehyde	-0.235	-0.706	-1.049	0.229
1-Chlorohexane	-0.181	-0.690	-1.104	0.321
1-Chlorooctane	0.415	-0.155	-0.617	0.979
p-Cresol	1.765	1.042	0.480	2.478
Cyclohexanone	1.013	0.477	0.028	1.543
Ethyl acetate	-0.205	-0.701	-1.129	0.283
Ethylbenzene	0.318	-0.224	-0.675	0.853
Methyl caproate	0.657	0.079	-0.397	1.227
Naphthalene	1.919	1.210	0.652	2.619
Nitrobenzene	1.664	1.027	0.515	2.292
1-Nitropropane	0.597	0.103	-0.313	1.084
1-Octanol	0.998	0.367	-0.173	1.621
Octylaldehyde	0.953	0.365	-0.141	1.534
1-Pentanol	0.132	-0.411	-0.823	0.667
2-Pentanone	0.279	-0.233	-0.630	0.785
Phenetole	1.014	0.414	-0.086	1.607
Phenol	1.449	0.785	0.270	2.104
Pyridine	0.438	-0.063	-0.465	0.932
m-Xylene	0.396	-0.153	-0.591	0.938
o-Xylene	0.503	-0.045	-0.490	1.044
p-Xylene	0.363	-0.185	-0.622	0.905
2-Propanol	-0.714			
1-Bromohexane	0.070	-0.460	-0.830	0.592

Propionic acid	0.374	-0.198	-0.600	0.937
1-Decanol	1.595	0.829	0.244	2.351

[a] Extrapolated values based on measured chromatographic retention data at 323 and 353 K.

Table 2. Chromatographic retention factor data for organic solutes on a $[BMPyrr]^+[Tri]^-$ stationary phase at 298 K, 323 K, 353 K and 383 K

Solute	$\log_{10} k$ (323 K)	$\log_{10} k$ (353 K)	$\log_{10} k$ (383 K)	$\log_{10} k$ (298 K)[a]
Acetic acid	1.838	1.167	0.655	2.501
Acetophenone	2.082	1.411	0.917	2.744
Benzaldehyde	1.792	1.124	0.624	2.451
Benzene	-0.008	-0.399		0.377
Benzonitrile	1.963	1.278	0.764	2.638
1-Bromooctane	0.960	0.352	-0.164	1.561
1-Butanol	0.858	0.288	-0.156	1.421
1-Chlorohexane	0.088	-0.432		0.601
1-Chlorooctane	0.675	0.106	-0.379	1.237
Cyclohexanol	1.617	0.918	0.380	2.307
Cyclohexanone	1.245	0.680	0.221	1.804
1,2-Dichlorobenzene	1.318	0.720	0.241	1.907
1,4-Dioxane	0.464	-0.004	-0.401	0.926
Ethyl acetate	-0.129			
Ethylbenzene	0.511	0.007	-0.433	1.009
1-Iodobutane	0.084	-0.351		0.514
Methyl caproate	0.707	0.140	-0.351	1.268
Naphthalene	2.260	1.478	0.879	3.031
Nitrobenzene	2.213	1.465	0.901	2.952
1-Nitropropane	0.983	0.456	0.031	1.503
1-Octanol	1.988	1.169	0.540	2.796
Octylaldehyde	1.091	0.470	-0.035	1.704
1-Pentanol	1.158	0.530	0.041	1.777
2-Pentanone	0.332	-0.119	-0.515	0.778
Phenetole	1.307	0.680	0.177	1.926
Propionitrile	0.499	0.072	-0.317	0.920
Pyrrole	1.949	1.268	0.755	2.620
Toluene	0.281	-0.170		0.727
m-Xylene	0.567	0.052	-0.392	1.074
o-Xylene	0.726	0.188	-0.263	1.257
p-Xylene	0.565	0.048	-0.396	1.075
2-Propanol	0.287	-0.206		0.773
2-Nitrophenol	2.450	1.645	1.028	3.244

1-Bromohexane	0.380	-0.113	-0.557	0.866
Propionic acid	2.051	1.320	0.755	2.772
1-Decanol	2.537	1.548	0.775	3.513
1-Chlorobutane	-0.472			
Butyraldehyde	-0.035			

[a] Extrapolated values based on measured chromatographic retention data at 323 and 353 K.

Table 3. Chromatographic retention factor data for organic solutes on a $[MeoeMMorp]^+[FAP]^-$ stationary phase at 298 K, 323 K, 353 K and 383 K

Solute	$\log_{10} k$ (323 K)	$\log_{10} k$ (353 K)	$\log_{10} k$ (383 K)	$\log_{10} k$ (298 K)[a]
Acetic acid	0.553	0.015	-0.423	1.085
Acetophenone	2.108	1.405	0.826	2.801
Benzaldehyde	1.590	0.961	0.816	2.210
Benzene	-0.136	-0.542	-0.916	0.265
Benzonitrile	1.736	1.110	0.594	2.353
Benzyl alcohol	2.150	1.394	0.786	2.897
1-Bromooctane	0.703	0.125	-0.356	1.274
1-Butanol	0.086	-0.366	-0.765	0.533
Butyraldehyde	0.051	-0.365	-0.750	0.462
1-Chlorohexane	-0.140	-0.570	-0.951	0.285
1-Chlorooctane	0.455	-0.091	-0.540	0.994
p-Cresol	2.011	1.282	0.689	2.731
Cyclohexanol	0.857	0.292	-0.172	1.414
Cyclohexanone	1.393	0.807	0.328	1.972
1,2-Dichlorobenzene	0.856	0.315	-0.126	1.389
1,4-Dioxane	0.616	0.085	-0.348	1.141
Ethyl acetate	0.135	-0.343	-0.735	0.607
Ethylbenzene	0.412	-0.110	-0.533	0.928
1-Iodobutane	-0.259	-0.666		0.142
Methyl caproate	0.909	0.302	-0.186	1.509
Naphthalene	2.076	1.388	0.812	2.756
Nitrobenzene	1.989	1.315	0.774	2.654
1-Nitropropane	0.921	0.389	-0.045	1.447
1-Octanol	1.219	0.548	0.015	1.881
Octylaldehyde	1.160	0.536	0.036	1.776
1-Pentanol	0.389	-0.138	-0.560	0.909
2-Pentanone	0.519	0.061	-0.353	0.971
Phenetole	1.188	0.560	0.057	1.808
Phenol	1.728	1.042	0.494	2.406
Propionitrile	0.565	0.099	-0.278	1.025
Pyridine	0.772	0.304	-0.154	1.235
Pyrrole	1.310	0.691	0.190	1.921
Toluene	0.186	-0.302	-0.689	0.667

m-Xylene	0.494	-0.046	-0.481	1.026
o-Xylene	0.614	0.066	-0.375	1.155
p-Xylene	0.459	-0.075	0.503	0.985
2-Propanol	-0.407	-0.835		0.016
2-Nitrophenol	1.960	1.259	0.697	2.652
1-Bromohexane	0.112	-0.373	-0.773	0.591
Propionic acid	0.792	0.193	-0.264	1.384
1-Decanol	1.780	1.007	0.395	2.542

[a] Extrapolated values based on measured chromatographic retention data at 323 and 353 K.

Table 4. Comparison of the extrapolated $\log_{10} k$ (298 K) values based on chromatographic retention factor data for solutes on a $[BMPyrr]^+[FAP]^-$ stationary phase measured at 323 and 353 K, and at 323 and 383 K.

Solute	$\log_{10} k$ (298 K)	$\log_{10} k$ (298 K)	Difference
	323 K and 353 K data	323 K and 383 K data	
Acetic acid	0.653	0.647	-0.006
Acetophenone	2.466	2.447	-0.019
Benzaldehyde	1.881	1.865	-0.015
Benzene	0.193	0.194	0.001
Benzonitrile	2.024	2.010	-0.014
Benzyl alcohol	2.406	2.387	-0.019
1-Bromooctane	1.220	1.225	0.005
1-Butanol	0.296	0.288	-0.008
Butyraldehyde	0.229	0.200	-0.029
2-Chloroaniline	2.564	2.545	-0.019
1-Chlorohexane	0.321	0.312	-0.009
1-Chlorooctane	0.979	0.968	-0.011
p-Cresol	2.478	2.453	-0.025
Cyclohexanone	1.543	1.541	-0.002
Ethyl Acetate	0.283	0.289	0.006
Ethyl benzene	0.853	0.850	-0.003
Methyl Caproate	1.227	1.221	-0.006
Naphthalene	2.619	2.597	-0.022
Nitrobenzene	2.292	2.279	-0.013
1-Nitropropane	1.084	1.084	-0.001
1-Octanol	1.621	1.625	0.004
Octylaldehyde	1.534	1.539	0.005
1-Pentanol	0.667	0.642	-0.025
2-Pentanone	0.785	0.766	-0.019
Phenetole	1.607	1.604	-0.003
Phenol	2.104	2.080	-0.024
Pyridine	0.932	0.921	-0.011
m-Xylene	0.938	0.924	-0.014

o-Xylene	1.044	1.035	-0.009
p-Xylene	0.905	0.891	-0.014
1-Bromohexane	0.592	0.552	-0.041
Propionic acid	0.937	0.895	-0.043
1-Decanol	2.351	2.319	-0.033

Table 5. Comparison of the extrapolated $\log_{10} k$ (298 K) values based on chromatographic retention factor data for solutes on a $[BMPyrr]^+[Tri]^-$ stationary phase measured at 323 and 353 K, and at 323 and 383 K.

Solute	$\log_{10} k$ (298 K)	$\log_{10} k$ (298)	Difference
	323 K and 353 K data		
Acetic acid	2.501	2.472	-0.029
Acetophenone	2.744	2.706	-0.038
Benzaldehyde	2.451	2.417	-0.034
Benzonitrile	2.638	2.605	-0.034
1-Bromooctane	1.561	1.562	0.001
1-Butanol	1.421	1.402	-0.019
1-Chlorooctane	1.237	1.239	0.003
Cyclohexanol	2.307	2.280	-0.028
Cyclohexanone	1.804	1.794	-0.010
1,2-Dichlorobenzene	1.907	1.894	-0.013
1,4-Dioxane	0.926	0.927	0.001
Ethyl benzene	1.009	1.017	0.007
Methyl Caproate	1.268	1.274	0.007
Naphthalene	3.031	2.999	-0.032
Nitrobenzene	2.952	2.916	-0.036
1-Nitropropane	1.503	1.493	-0.010
1-Octanol	2.796	2.763	-0.033
Octylaldehyde	1.704	1.694	-0.010
1-Pentanol	1.777	1.756	-0.021
2-Pentanone	0.778	0.786	0.008
Phenetole	1.926	1.912	-0.014
Propionitrile	0.920	0.936	0.016
Pyrrole	2.620	2.587	-0.033
m-Xylene	1.074	1.080	0.005
o-Xylene	1.257	1.256	-0.001
p-Xylene	1.075	1.080	0.004
2-Nitrophenol	3.244	3.211	-0.033
1-Bromohexane	0.866	0.881	0.015
Propionic acid	2.772	2.745	-0.028
1-Decanol	3.513	3.480	-0.033

Table 6. Comparison of the extrapolated $\log_{10} k$ (298 K) values based on chromatographic retention factor data for solutes on a $[MeoeMMorp]^+[FAP]^-$ stationary phase measured at 323 and 353 K, and at 323 and 383 K.

Solute	$\log_{10} k$ (298 K)	$\log_{10} k$ (298 K)	Difference
	323 K and 353 K data	353 K and 383 K data	
Acetic acid	1.085	1.076	-0.009
Acetophenone	2.801	2.794	-0.007
Aniline	2.840	2.833	-0.007
Benzaldehyde	2.210	2.201	-0.009
Benzene	0.265	0.282	0.017
Benzonitrile	2.353	2.347	-0.006
Benzyl alcohol	2.897	2.881	-0.016
1-Bromooctane	1.274	1.271	-0.004
1-Butanol	0.533	0.542	0.009
Butyraldehyde	0.462	0.480	0.018
2-Chloroaniline	2.826	2.829	0.002
1-Chlorohexane	0.285	0.295	0.010
1-Chlorooctane	0.994	0.988	-0.006
p-Cresol	2.731	2.720	-0.012
Cyclohexanol	1.414	1.408	-0.006
Cyclohexanone	1.972	1.964	-0.008
1,2-Dichlorobenzene	1.389	1.381	-0.008
1,4-Dioxane	1.141	1.133	-0.008
Ethyl Acetate	0.607	0.600	-0.007
Ethyl benzene	0.928	0.918	-0.009
Methyl Caproate	1.509	1.496	-0.013
Naphthalene	2.756	2.753	-0.002
Nitrobenzene	2.654	2.639	-0.015
1-Nitropropane	1.447	1.439	-0.008
1-Octanol	1.881	1.864	-0.017
Octylaldehyde	1.776	1.762	-0.014
1-Pentanol	0.909	0.897	-0.012
2-Pentanone	0.971	0.986	0.014
Phenetole	1.808	1.794	-0.014
Phenol	2.406	2.389	-0.016
Propionitrile	1.025	1.017	-0.008

Pyridine	1.235	1.268	0.034
Pyrrole	1.921	1.910	-0.011
Toluene	0.667	0.654	-0.014
m-Xylene	1.026	1.015	-0.011
o-Xylene	1.155	1.143	-0.012
p-Xylene	0.985	0.974	-0.011
2-Nitrophenol	2.652	2.636	-0.016
1-Bromohexane	0.591	0.586	-0.005
Propionic acid	1.384	1.357	-0.026
1-Decanol	2.542	2.521	-0.021

Table 7. Logarithm of gas-to-anhydrous IL partition coefficient, $\log_{10} K$, and logarithm of water-to-anhydrous IL partition coefficient, $\log_{10} P$, for organic solutes dissolved in $[BMPyrr]^+[FAP]^-$ at 298 K and 323 K

Solute	$\log_{10} K$ (298 K)	$\log_{10} K$ (323 K)	$\log_{10} P$ (298 K)
Calculated from Activity Coefficient Data:			
Pentane	1.056	0.817	2.756
Hexane	1.448	1.132	3.268
3-Methylpentane	1.398	1.105	3.238
2,2-Dimethylbutane	1.218	0.965	3.058
Heptane	1.800	1.437	3.760
Octane	2.150	1.735	4.260
2,2,4-Trimethylpentane	1.826	1.463	3.946
Nonane	2.495	2.029	4.645
Decane	2.837	2.322	5.157
Cyclohexane	1.793	1.469	2.693
Methylcyclohexane	2.001	1.645	3.251
Cycloheptane	2.289	1.900	2.869
Cyclooctane	2.740	2.287	3.510
1-Hexene	1.661	1.339	2.821
Cyclohexene	2.084	1.722	2.354
1-Heptene	2.026	1.637	3.246
1-Octene	2.374	1.935	3.784
1-Decene	3.099	2.515	4.739
1-Hexyne	2.144	1.763	2.354
1-Heptyne	2.613	2.067	3.053
1-Octyne	2.871	2.363	3.391
Benzene	2.979	2.529	2.349
Toluene	3.379	2.867	2.729
Ethylbenzene	3.670	3.116	3.090
o-Xylene	3.887	3.312	3.227
m-Xylene	3.773	3.200	3.163
p-Xylene	3.733	3.163	3.143
Styrene	4.060	3.466	3.110
α-Methylstyrene	4.305	3.636	3.345
Methanol	2.045	1.743	-1.695

Ethanol	2.338	1.959	-1.332
1-Propanol	2.687	2.258	-0.873
2-Propanol	2.442	2.061	-1.038
1-Butanol	3.073	2.579	-0.387
2-Butanol	2.788	2.346	-0.602
2-Methyl-1-propanol	2.877	2.422	-0.413
Acetic acid	3.311	2.773	-1.599
Thiophene	3.017	2.561	1.977
Tetrahydrofuran	2.865	2.432	0.315
1,4-Dioxane	3.533	3.022	-0.177
Methyl *tert*-butyl ether	2.199	1.803	0.579
Ethyl *tert*-butyl ether	2.105	1.705	0.835
Methyl *tert*-amyl ether	2.546	2.100	1.076
Diethyl ether	1.823	1.493	0.653
Dipropyl ether	2.349	1.925	1.459
Diisopropyl ether	2.036	1.648	0.968
Dibutyl ether	3.012	2.477	2.322
Acetone	2.942	2.543	0.152
2-Pentanone	3.585	3.074	1.005
3-Pentanone	3.586	3.073	1.085
Methyl acetate	2.787	2.369	0.487
Ethyl acetate	3.067	2.596	0.907
Methyl propanoate	3.114	2.644	0.964
Methyl butanoate	3.417	2.894	1.337
Butyraldehyde	3.000	2.566	0.670
Acetonitrile	3.226	2.827	0.376
Pyridine	3.769	3.245	0.329
1-Nitropropane	3.979	3.435	1.529
Calculated from Retention Factor Data:			
Acetophenone	5.268	4.579	1.908
Acetic acid	3.455	2.891	-1.455
Benzaldehyde	4.683	4.075	1.733
Benzene	2.995	2.515	2.365
Benzonitrile	4.826	4.222	1.736
Benzyl alcohol	5.208	4.507	0.348
1-Bromooctane	4.022	3.438	4.402
1-Butanol	3.098	2.587	-0.362
Butyraldehyde	3.031	2.555	0.701

1-Chlorohexane	3.123	2.609	3.123
1-Chlorooctane	3.781	3.205	3.971
p-Cresol	5.280	4.555	0.780
Cyclohexanone	4.345	3.803	0.745
Ethyl acetate	3.085	2.585	0.925
Ethylbenzene	3.655	3.108	3.075
Methyl caproate	4.029	3.447	2.199
Naphthalene	5.421	4.709	3.691
Nitrobenzene	5.094	4.454	2.074
1-Nitropropane	3.886	3.387	1.436
1-Octanol	4.423	3.788	1.423
Octylaldehyde	4.336	3.743	2.656
1-Pentanol	3.469	2.922	0.119
2-Pentanone	3.587	3.069	1.007
Phenetole	4.409	3.804	2.779
Phenol	4.906	4.239	0.056
Pyridine	3.734	3.228	0.294
m-Xylene	3.740	3.186	3.130
o-Xylene	3.846	3.293	3.186
p-Xylene	3.707	3.153	3.117
1-Bromohexane	3.394	2.860	3.524
Propionic acid	3.739	3.164	-1.001
1-Decanol	5.153	4.385	2.483
2-Propanol		2.076	

Table 8. Logarithm of gas-to-anhydrous IL partition coefficient, $\log_{10} K$, and logarithm of water-to-anhydrous IL partition coefficient, $\log_{10} P$, for organic solutes dissolved in $[BMPyrr]^+[Trif]^-$ at 298 K and 323 K

Solute	$\log_{10} K$ (298 K)	$\log_{10} K$ (323 K)	$\log_{10} P$ (298 K)
Calculated from Activity Coefficient Data:			
Pentane	0.475	0.245	2.175
Hexane	0.973	0.648	2.793
Heptane	1.390	1.000	3.350
Octane	1.776	1.321	3.886
Nonane	2.133	1.622	4.283
Decane	2.479	1.907	4.799
Cyclopentane	1.117	0.828	1.997
Cyclohexane	1.502	1.157	2.402
Cycloheptane	2.096	1.668	2.676
Cyclooctane	2.578	2.089	3.348
1-Pentene	0.851	0.572	2.081
1-Hexene	1.300	0.948	2.460
1-Heptene	1.689	1.268	2.909
1-Octene	2.048	1.574	3.458
1-Pentyne	1.850	1.434	1.860
1-Hexyne	2.216	1.756	2.426
1-Heptyne	2.669	2.048	3.109
1-Octyne	2.914	2.334	3.434
Benzene	2.776	2.302	2.146
Toluene	3.112	2.590	2.462
Ethylbenzene	3.385	2.817	2.805
σ-Xylene	3.618	3.026	2.958
m-Xylene	3.443	2.868	2.833
p-Xylene	3.442	2.863	2.852
Methanol	2.945	2.473	-0.795
Ethanol	3.107	2.587	-0.563
1-Propanol	3.451	2.870	-0.109
1-Butanol	3.821	3.192	0.351
Tetrahydrofuran	2.554	2.109	0.004
Thiophene	2.996	2.506	1.956

Methyl *tert*-butyl ether	1.750	1.345	0.130
Calculated from Retention Factor Data:			
Acetophenone	5.123	4.390	1.763
Acetic acid	4.880	4.146	-0.030
Benzaldehyde	4.830	4.100	1.880
Benzene	2.756	2.300	2.126
Benzonitrile	5.017	4.271	1.927
1-Bromooctane	3.940	3.268	4.320
1-Butanol	3.800	3.166	0.340
1-Chlorohexane	2.980	2.396	2.980
1-Chlorooctane	3.616	2.983	3.806
Cyclohexanol	4.686	3.925	0.676
Cyclohexanone	4.183	3.553	0.583
1,2-Dichlorobenzene	4.286	3.626	3.386
1,4-Dioxane	3.305	2.772	-0.405
Ethylbenzene	3.388	2.819	2.808
1-Iodobutane	2.893	2.392	2.713
Methyl caproate	3.647	3.015	1.817
Naphthalene	5.410	4.568	3.680
Nitrobenzene	5.331	4.521	2.311
1-Nitropropane	3.882	3.291	1.432
1-Octanol	5.175	4.296	2.175
Octylaldehyde	4.083	3.399	2.403
1-Pentanol	4.156	3.466	0.806
2-Pentanone	3.157	2.640	0.577
Phenetole	4.305	3.615	2.675
Propionitrile	3.299	2.807	0.479
Pyrrole	4.999	4.257	
Toluene	3.106	2.589	2.456
m-Xylene	3.453	2.875	2.843
o-Xylene	3.636	3.034	2.976
p-Xylene	3.454	2.873	2.864
1-Bromohexane	3.245	2.688	3.375
Propionic acid	5.151	4.359	0.411
1-Decanol	5.892	4.845	3.222
2-Nitrophenol	5.623	4.758	2.263
2-Propanol	3.152	2.595	-0.328

Butyraldehyde		2.273	
1-Chlorobutane		1.836	
Ethyl acetate		2.179	

Table 9. Logarithm of gas-to-anhydrous IL partition coefficient, $\log_{10} K$, and logarithm of water-to-anhydrous IL partition coefficient, $\log_{10} P$, for organic solutes dissolved in $[MeoeMMorp]^+[FAP]^-$ at 298 K and 323 K

Solute	$\log_{10} K$ (298 K)	$\log_{10} K$ (323 K)	$\log_{10} P$ (298)
Calculated from Activity Coefficient Data:			
Pentane	0.791	0.557	2.491
Hexane	1.147	0.853	2.967
3-Methylpentane	1.098	0.827	2.938
2,2-Dimethylbutane	0.921	0.681	2.761
Heptane	1.478	1.137	3.438
Octane	1.820	1.421	3.930
2,2,4-Trimethylpentane	1.482	1.153	3.602
Nonane	2.151	1.699	4.301
Decane	2.493	1.979	4.813
Cyclopentane	1.222	0.959	2.102
Cyclohexane	1.539	1.227	2.439
Methylcyclohexane	1.722	1.384	2.972
Cycloheptane	2.022	1.653	2.602
Cyclooctane	2.457	2.031	3.227
1-Pentene	1.079	0.812	2.309
1-Hexene	1.426	1.104	2.586
Cyclohexene	1.886	1.533	2.156
1-Heptene	1.765	1.385	2.985
1-Octene	2.084	1.660	3.494
1-Decene	2.721	2.022	4.361
1-Pentyne	1.682	1.339	1.692
1-Hexyne	2.012	1.619	2.222
1-Heptyne	2.339	1.898	2.779
1-Octyne	2.651	2.167	3.171
Benzene	2.894	2.417	2.264
Toluene	3.257	2.727	2.607
Ethylbenzene	3.522	2.950	2.942
o-Xylene	3.751	3.155	3.091
m-Xylene	3.617	3.033	3.007
p-Xylene	3.577	2.998	2.987
Styrene	3.949	3.332	2.999
α-Methylstyrene	4.136	3.479	3.176

Methanol	2.328	1.913	-1.412
Ethanol	2.535	2.097	-1.135
1-Propanol	2.848	2.360	-0.712
2-Propanol	2.628	2.157	-0.852
1-Butanol	3.197	2.660	-0.263
2-Butanol	2.930	2.414	-0.460
2-Methyl-1-propanol	3.016	2.493	-0.284
2-Methyl-2-propanol	2.686	2.190	-0.594
Thiophene	2.962	2.480	1.922
Tetrahydrofuran	2.951	2.474	0.401
1,4-Dioxane	3.760	3.177	0.050
Methyl *tert*-butyl ether	2.152	1.744	0.532
Ethyl *tert*-butyl ether	1.969	1.565	0.699
Methyl *tert*-amyl ether	2.463	2.008	0.993
Diethyl ether	1.801	1.440	0.631
Dipropyl ether	2.216	1.785	1.326
Diisopropyl ether	1.903	1.504	0.853
Dibutyl ether	2.799	2.281	2.109
Acetone	3.194	2.705	0.404
2-Pentanone	3.723	3.152	1.143
3-Pentanone	3.710	3.135	1.210
Methyl acetate	3.019	2.522	0.719
Ethyl Acetate	3.249	2.711	1.089
Methyl propanoate	3.276	2.736	1.126
Methyl butanoate	3.524	2.947	1.444
Butyraldehyde	3.116	2.631	0.786
Acetonitrile	3.463	2.984	0.613
Pyridine	3.849	3.287	0.409
1-Nitropropane	4.071	3.485	1.621
Calculated from Retention Factor Data:			
Acetophenone	5.420	4.665	2.060
Acetic acid	3.704	3.110	-1.206
Benzaldehyde	4.829	4.147	1.879
Benzene	2.884	2.421	2.254
Benzonitrile	4.972	4.293	1.882
Benzyl alcohol	5.516	4.707	0.656
1-Bromooctane	3.893	3.260	4.273
1-Butanol	3.152	2.643	-0.308
1-Chlorohexane	2.904	2.417	2.904

1-Chlorooctane	3.613	3.012	3.803
p-Cresol	5.350	4.568	0.850
Cyclohexanol	4.033	3.414	0.023
Cyclohexanone	4.591	3.950	0.991
1,2-Dichlorobenzene	4.008	3.413	3.108
1,4-Dioxane	3.760	3.173	0.050
Ethylbenzene	3.547	2.969	2.967
1-Iodobutane	2.761	2.298	2.581
Methyl caproate	4.128	3.466	2.298
Naphthalene	5.375	4.633	3.645
Nitrobenzene	5.273	4.546	2.253
1-Nitropropane	4.066	3.478	1.616
1-Octanol	4.500	3.776	1.500
Octylaldehyde	4.395	3.717	2.715
1-Pentanol	3.528	2.946	0.178
2-Pentanone	3.590	3.076	1.010
Phenetole	4.427	3.745	2.797
Phenol	5.025	4.285	0.175
Propionitrile	3.644	3.122	0.824
Toluene	3.286	2.743	2.636
m-Xylene	3.645	3.051	3.035
o-Xylene	3.774	3.171	3.114
p-Xylene	3.604	3.016	3.014
1-Bromohexane	3.210	2.669	3.337
Propionic acid	4.003	3.349	-0.737
1-Decanol	5.161	4.337	2.491
2-Propanol	2.635	2.150	-0.845
Pyridine	3.854	3.329	0.414
Ethyl Acetate	3.226	2.692	1.066
Butyraldhedye		2.608	
Pyrrole		3.867	

Table 10. Abraham model solute descriptors of the organic compounds considered in the present study.

Solute	**E**	**S**	**A**	**B**	**L**	**V**
Pentane	0.000	0.000	0.000	0.000	2.162	0.8131
Hexane	0.000	0.000	0.000	0.000	2.668	0.9540
3-Methylpentane	0.000	0.000	0.000	0.000	2.581	0.9540
2,2-Dimethylbutane	0.000	0.000	0.000	0.000	2.352	0.9540
Heptane	0.000	0.000	0.000	0.000	3.173	1.0949
Octane	0.000	0.000	0.000	0.000	3.677	1.2358
2,2,4-Trimethylpentane	0.000	0.000	0.000	0.000	3.106	1.2358
Nonane	0.000	0.000	0.000	0.000	4.182	1.3767
Decane	0.000	0.000	0.000	0.000	4.686	1.5176
Cyclohexane	0.305	0.100	0.000	0.000	2.964	0.8454
Methylcyclohexane	0.244	0.060	0.000	0.000	3.319	0.9863
Cycloheptane	0.350	0.100	0.000	0.000	3.704	0.9863
Cyclooctane	0.413	0.100	0.000	0.000	4.329	1.1272
1-Pentene	0.093	0.080	0.000	0.070	2.047	0.7701
1-Hexene	0.078	0.080	0.000	0.070	2.572	0.9110
Cyclohexene	0.395	0.280	0.000	0.090	2.952	0.8204
1-Heptene	0.092	0.080	0.000	0.070	3.063	1.0519
1-Octene	0.094	0.080	0.000	0.070	3.568	1.1928
1-Decene	0.093	0.080	0.000	0.070	4.554	1.4746
1-Pentyne	0.172	0.230	0.120	0.120	2.010	0.7271
1-Hexyne	0.166	0.220	0.100	0.120	2.510	0.8680
1-Heptyne	0.160	0.230	0.120	0.100	3.000	1.0089
1-Octyne	0.155	0.220	0.090	0.100	3.521	1.1498
Benzene	0.610	0.520	0.000	0.140	2.786	0.7164
Toluene	0.601	0.520	0.000	0.140	3.325	0.8573
Ethylbenzene	0.613	0.510	0.000	0.150	3.778	0.9982
o-Xylene	0.663	0.560	0.000	0.160	3.939	0.9982
m-Xylene	0.623	0.520	0.000	0.160	3.839	0.9982
p-Xylene	0.613	0.520	0.000	0.160	3.839	0.9982
Styrene	0.849	0.650	0.000	0.160	3.908	0.9550
α-Methylstyrene	0.851	0.640	0.000	0.190	4.290	1.0960
Methanol	0.278	0.440	0.430	0.470	0.970	0.3082
Ethanol	0.246	0.420	0.370	0.480	1.485	0.4491

1-Propanol	0.236	0.420	0.370	0.480	2.031	0.5900
2-Propanol	0.212	0.360	0.330	0.560	1.764	0.5900
1-Butanol	0.224	0.420	0.370	0.480	2.601	0.7310
2-Butanol	0.217	0.360	0.330	0.560	2.338	0.7310
2-Methyl-1-propanol	0.217	0.390	0.370	0.480	2.413	0.7310
2-Methyl-2-propanol	0.180	0.300	0.310	0.600	1.963	0.7310
1-Pentanol	0.219	0.420	0.370	0.480	3.106	0.8718
1-Octanol	0.199	0.420	0.370	0.480	4.619	1.2950
1-Decanol	0.191	0.420	0.370	0.480	5.610	1.5763
Acetic acid	0.265	0.640	0.620	0.440	1.816	0.4648
Propionic acid	0.233	0.650	0.600	0.450	2.290	0.6057
Thiophene	0.687	0.570	0.000	0.150	2.819	0.6411
Tetrahydrofuran	0.289	0.520	0.000	0.480	2.636	0.6223
1,4-Dioxane	0.329	0.750	0.000	0.640	2.892	0.6810
Methyl *tert*-butyl ether	0.024	0.220	0.000	0.550	2.372	0.8718
Ethyl *tert*-butyl ether	-0.020	0.180	0.000	0.590	2.699	1.0127
Methyl *tert*-amyl ether	0.050	0.210	0.000	0.600	2.916	1.0127
Diethyl ether	0.041	0.250	0.000	0.450	2.015	0.7309
Dipropyl ether	0.008	0.250	0.000	0.450	2.954	1.0127
Diisopropyl ether	-0.063	0.170	0.000	0.570	2.501	1.0127
Dibutyl ether	0.000	0.250	0.000	0.450	3.924	1.2945
Acetone	0.179	0.700	0.040	0.490	1.696	0.5470
2-Pentanone	0.143	0.680	0.000	0.510	2.755	0.8288
3-Pentanone	0.154	0.660	0.000	0.510	2.811	0.8288
Methyl acetate	0.142	0.640	0.000	0.450	1.911	0.6057
Ethyl acetate	0.106	0.620	0.000	0.450	2.314	0.7466
Methyl propanoate	0.128	0.600	0.000	0.450	2.431	0.7470
Methyl butanoate	0.106	0.600	0.000	0.450	2.943	0.8880
Butyraldehdye	0.187	0.650	0.000	0.450	2.270	0.6880
Acetonitrile	0.237	0.900	0.070	0.320	1.739	0.4042
Pyridine	0.631	0.840	0.000	0.520	3.022	0.6750
1-Nitropropane	0.242	0.950	0.000	0.310	2.894	0.7055
Acetophenone	0.818	1.010	0.000	0.480	4.501	1.0139
Benzaldehyde	0.820	1.000	0.000	0.390	4.008	0.8730
Benzonitrile	0.742	1.110	0.000	0.330	4.039	0.8711
Benzyl alcohol	0.803	0.870	0.330	0.560	4.221	0.9160
1-Bromooctane	0.339	0.400	0.000	0.120	5.143	1.4108
Butyraldehyde	0.187	0.650	0.000	0.450	2.270	0.6880

1-Chlorohexane	0.201	0.390	0.000	0.090	3.708	1.0764
1-Chlorooctane	0.191	0.400	0.000	0.090	4.708	1.3582
p-Cresol	0.820	0.870	0.570	0.310	4.312	0.9160
Cyclohexanol	0.460	0.540	0.320	0.570	3.758	0.9040
Cyclohexanone	0.403	0.860	0.000	0.560	3.792	0.8611
1,2-Dichlorobenzene	0.872	0.780	0.000	0.040	4.318	0.9612
Methyl caproate	0.080	0.600	0.000	0.450	3.874	1.1693
Naphthalene	1.340	0.920	0.000	0.200	5.161	1.0854
Nitrobenzene	0.871	1.110	0.000	0.280	4.557	0.8906
Octylaldehyde	0.160	0.650	0.000	0.450	4.380	1.2515
Phenetole	0.681	0.700	0.000	0.320	4.242	1.0569
Phenol	0.805	0.890	0.600	0.300	3.766	0.7751
1-Bromohexane	0.349	0.400	0.000	0.120	4.130	1.1290
Pyrrole	0.613	0.730	0.410	0.290	2.865	0.5770
1-Iodobutane	0.628	0.400	0.000	0.150	3.628	0.9304
1-Chlorobutane	0.210	0.400	0.000	0.100	2.722	0.7946

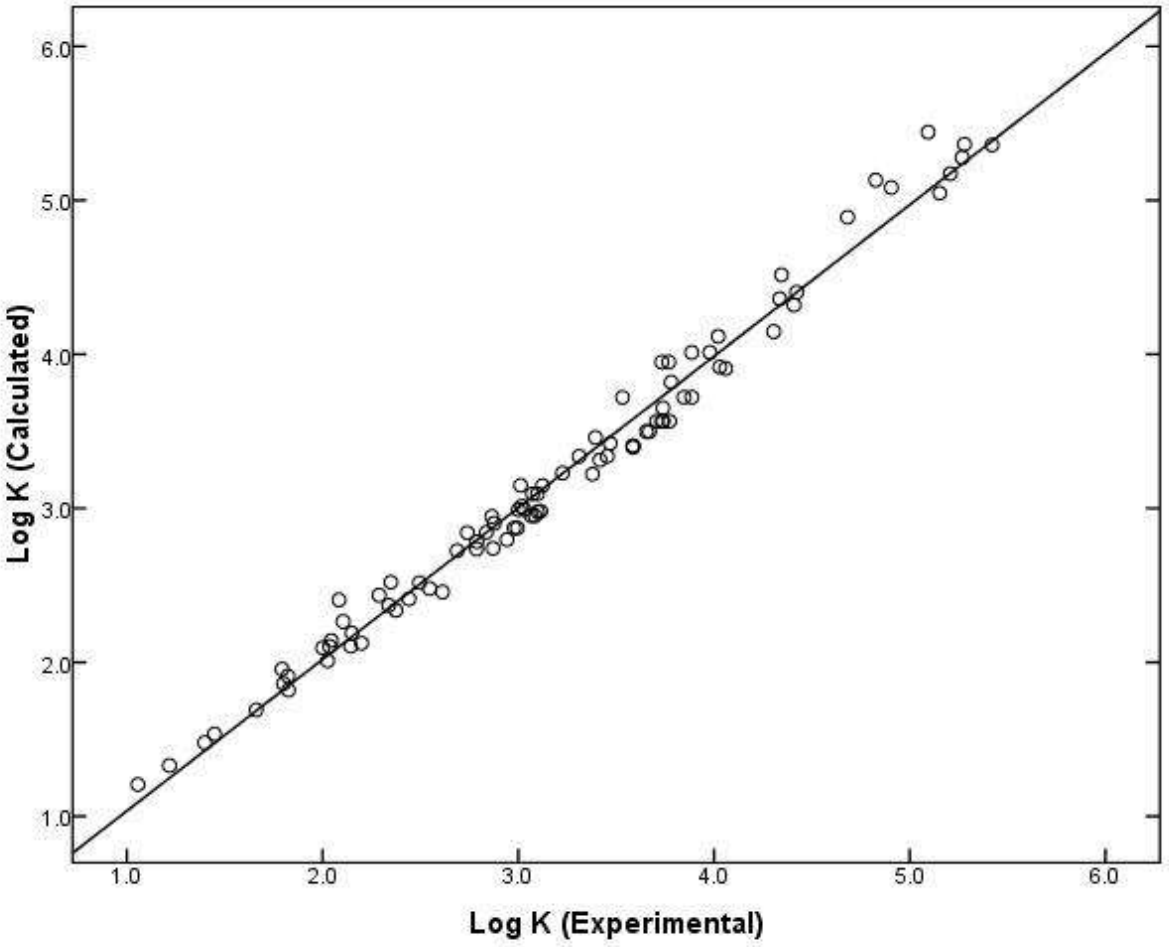

Figure 1. Comparison of experimental $\log_{10} K$ data versus calculated values based on eq 8 for $[BMPyrr]^+[FAP]^-$.

Figure 2

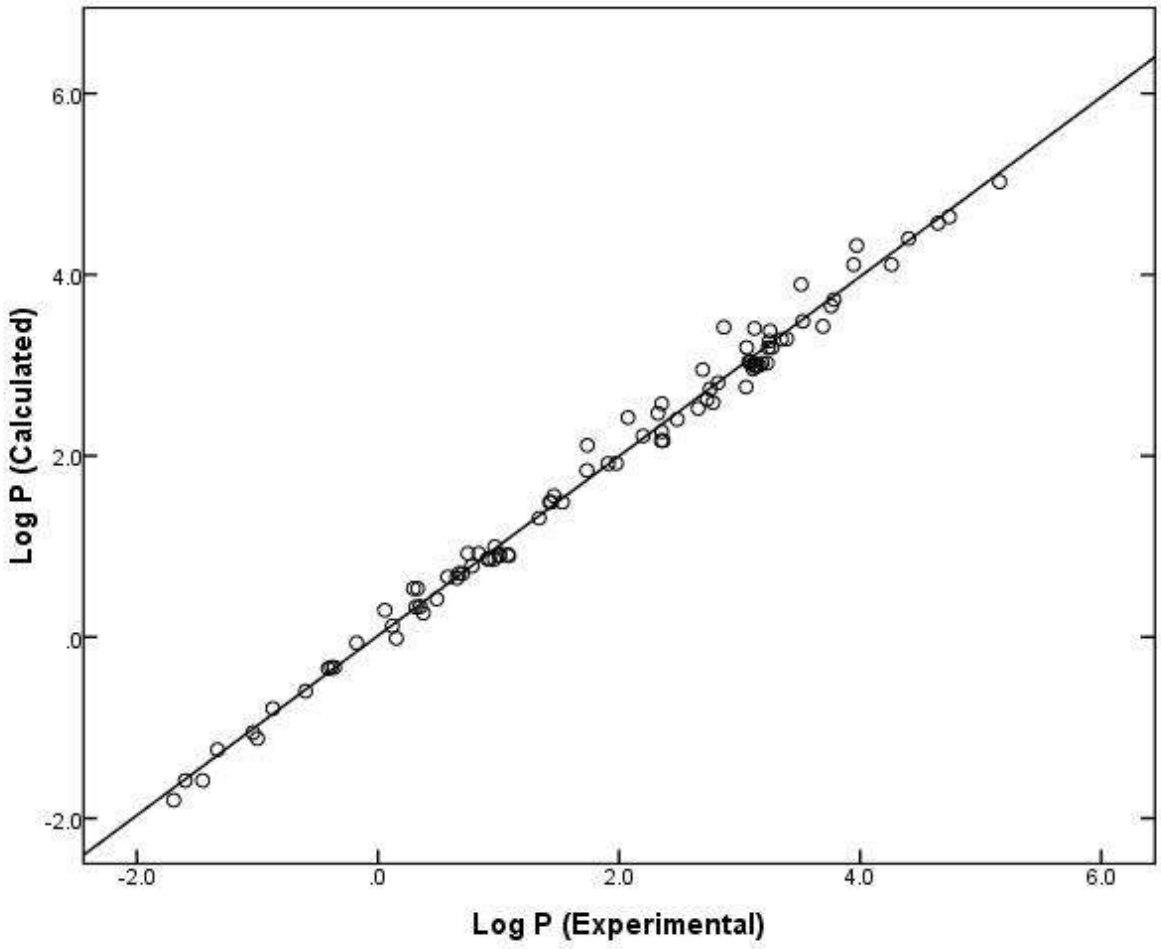

Figure 2. Comparison of experimental $\log_{10} P$ data versus calculated values based on eq 10 for $[BMPyrr]^{+}[FAP]^{-}$.

Figure 3

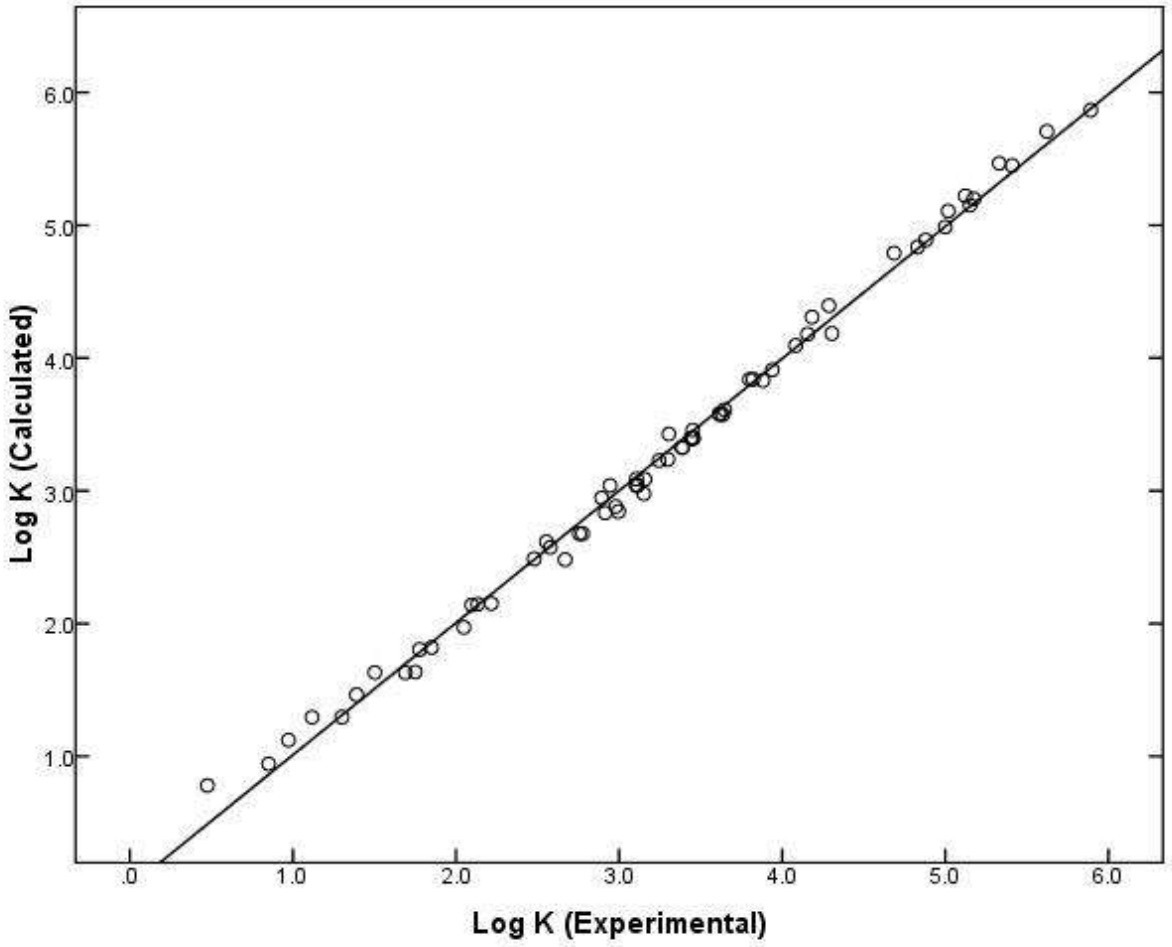

Figure 3. Comparison of experimental $\log_{10} K$ data versus calculated values based on eq 12 for $[BMPyrr]^+[Trif]^-$.

Figure 4

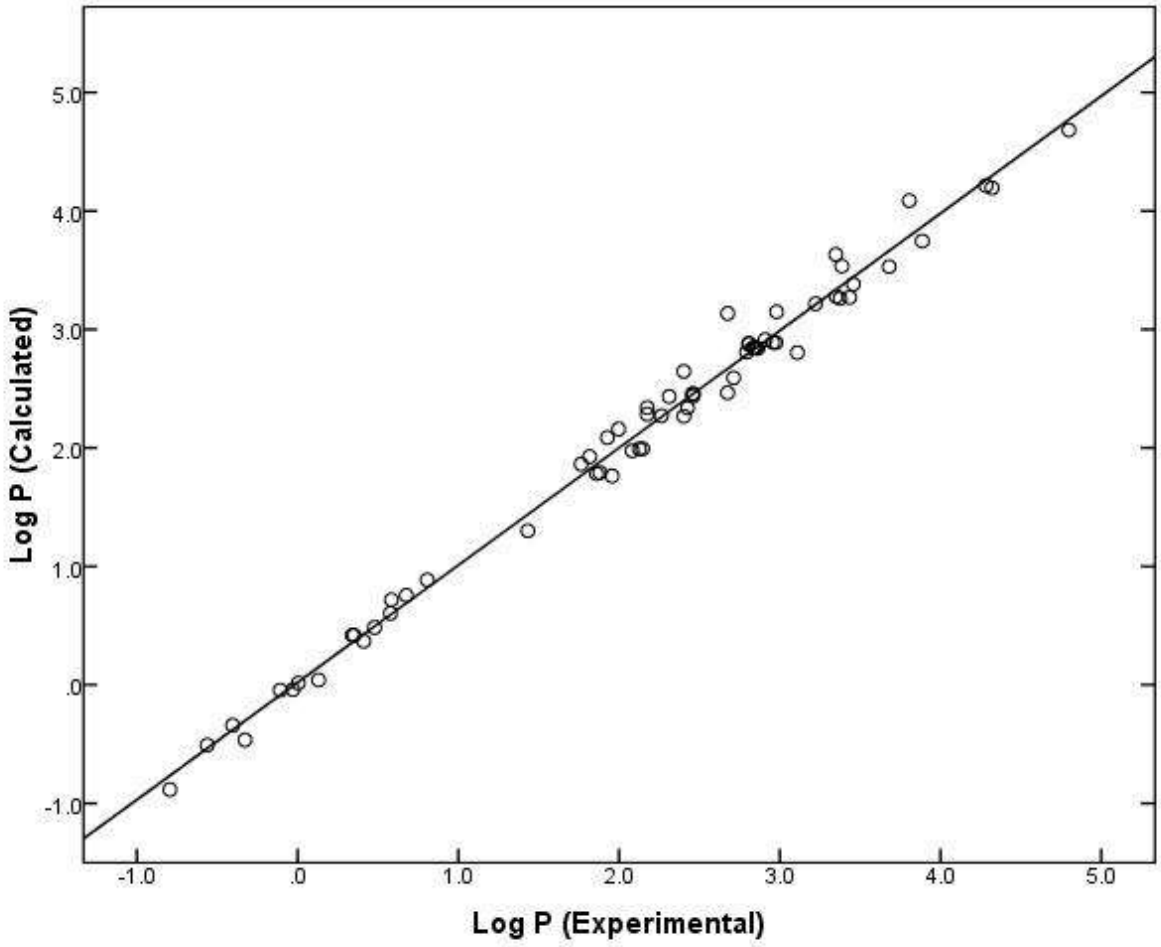

Figure 4. Comparison of experimental $\log_{10} P$ data versus calculated values based on eq 14 for $[BMPyrr]^+[Trif]^-$.

Figure 5

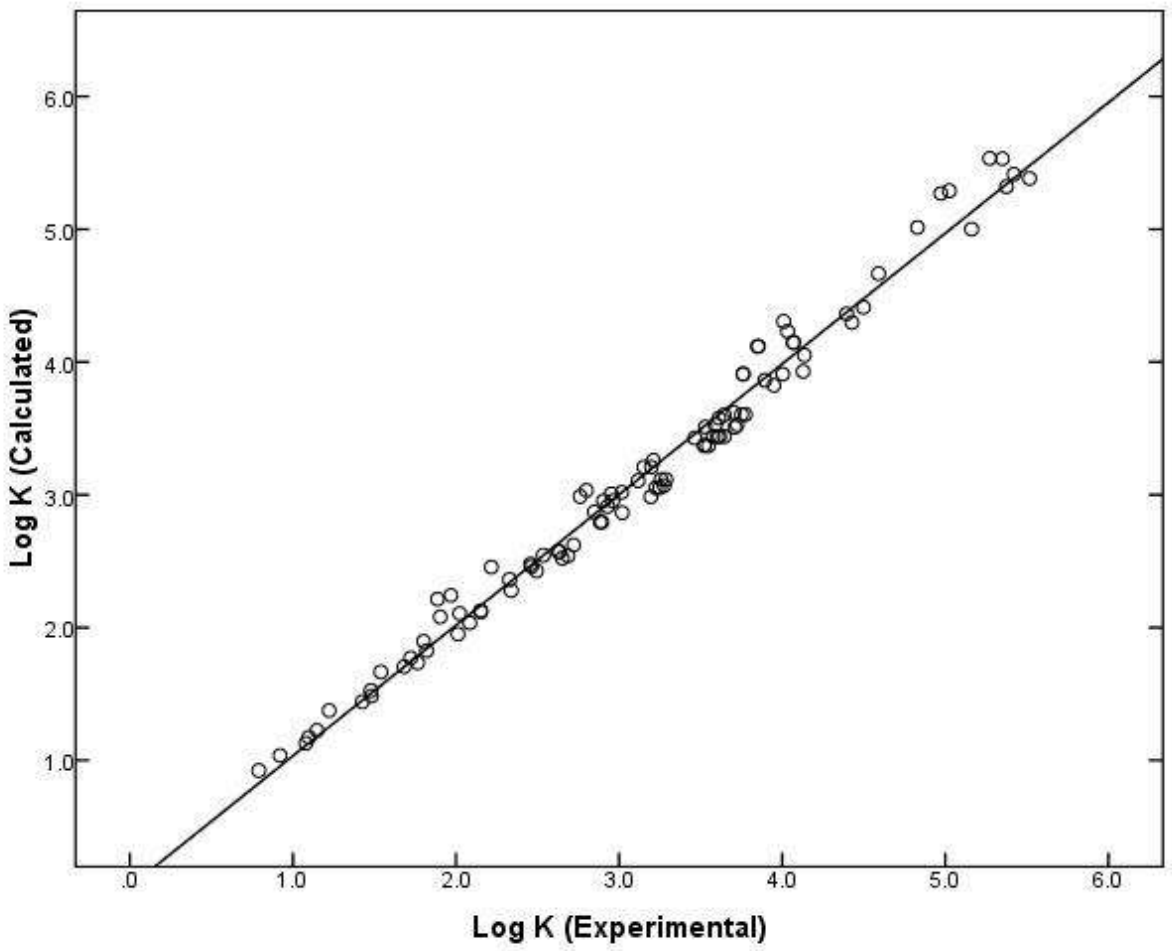

Figure 5. Comparison of experimental $\log_{10} K$ data versus calculated values based on eq 18 for $[MeoeMMorp]^+[FAP]^-$.

Figure 6

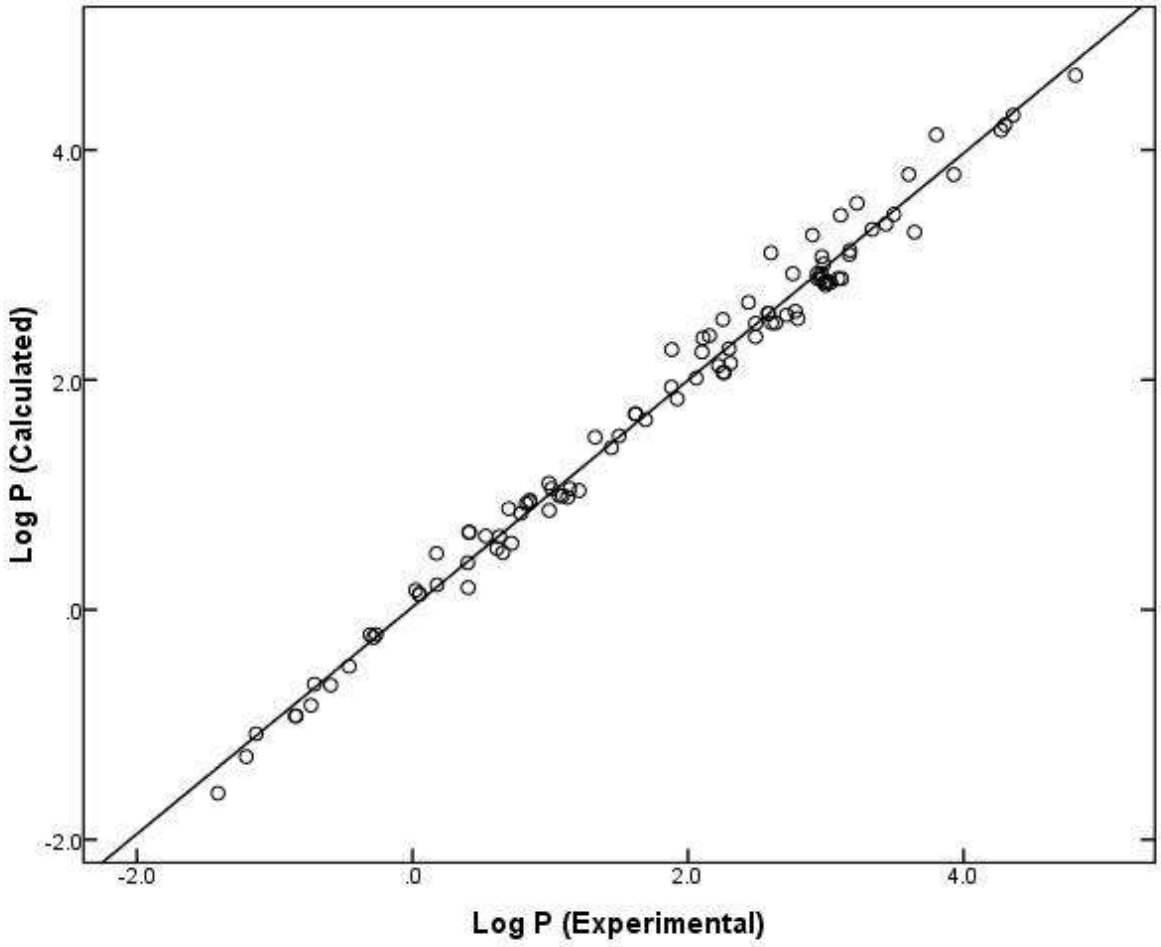

Figure 6. Comparison of experimental $\log_{10} P$ data versus calculated values based on eq 20 for $[MeoeMMorp]^{+}[FAP]^{-}$.